JGR Atmospheres

RESEARCH ARTICLE
10.1029/2022JD038099

Special Section:
Advances in scaling and modeling of land-atmosphere interactions

Exploring the Meteorological Impacts of Surface and Rooftop Heat Mitigation Strategies Over a Tropical City

Ansar Khan[1], Samiran Khorat[2], Quang-Van Doan[3], Rupali Khatun[2], Debashish Das[4], Rafiq Hamdi[5], Laura Carlosena[6], Mattheos Santamouris[7], Matei Georgescu[8], and Dev Niyogi[9,10]

[1]Department of Geography, Lalbaba College, University of Calcutta, Kolkata, India, [2]School of Environmental Studies, Jadavpur University, Kolkata, India, [3]Centre for Computational Sciences, University of Tsukuba, Tsukuba, Japan, [4]Department of Architecture, Jadavpur University, Kolkata, India, [5]Royal Meteorological Institute of Belgium, Brussels, Belgium, [6]Department of Engineering, Public University of Navarre (UPNA), Pamplona, Spain, [7]Faculty of Built Environment, University of New South Wales, Sydney, NSW, Australia, [8]School of Geographical Sciences and Urban Planning, Arizona State University, Tempe, AZ, USA, [9]Department of Geological Sciences, Jackson School of Geosciences, The University of Texas at Austin, Austin, TX, USA, [10]Department of Civil, Architectural, and Environmental Engineering, The University of Texas at Austin, Austin, TX, USA

Abstract Different heat mitigation technologies have been developed to improve the thermal environment in cities. However, the regional impacts of such technologies, especially in the context of a tropical city, remain unclear. The deployment of heat mitigation technologies at city-scale can change the radiation balance, advective flow, and energy balance between urban areas and the overlying atmosphere. We used the mesoscale Weather Research and Forecasting model coupled with a physically based single-layer urban canopy model to assess the impacts of five different heat mitigation technologies on surface energy balance, standard surface meteorological fields, and planetary boundary layer (PBL) dynamics for premonsoon typical hot summer days over a tropical coastal city in the month of April in 2018, 2019, and 2020. Results indicate that the regional impacts of cool materials (CMs), super-cool broadband radiative coolers, green roofs (GRs), vegetation fraction change, and a combination of CMs and GRs (i.e., "Cool city (CC)") on the lower atmosphere are different at diurnal scale. Results showed that super-cool materials have the maximum potential of ambient temperature reduction of 1.6°C during peak hour (14:00 LT) compared to other technologies in the study. During the daytime hours, the PBL height was considerably lower than the reference scenario with no implementation of strategies by 700 m for super-cool materials and 500 m for both CMs and CC cases; however, the green roofing system underwent nominal changes over the urban area. During the nighttime hours, the PBL height increased by CMs and the CC strategies compared to the reference scenario, but minimal changes were evident for super-cool materials. The changes of temperature on the vertical profile of the heat mitigation implemented city reveal a stable PBL over the urban domain and a reduction of the vertical mixing associated with a pollution dome. This would lead to crossover phenomena above the PBL due to the decrease in vertical wind speed. Therefore, assessing the coupled regional impact of urban heat mitigation over the lower atmosphere at city-scale is urgent for sustainable urban planning.

Plain Language Summary In this research we evaluated the impact on the city meteorology and on the lower atmosphere due to the use of several heat mitigation technologies. The numerical simulations were carried out during typical summer hot days over an Indian tropical city. The heat mitigation strategies considered include very reflective materials (cool materials (CMs), super-cool broadband radiative coolers) green roofs (GRs), changes in the vegetation fraction, and a combination of CMs and GRs (i.e., cool city (CC)). In particular, these mitigation strategies and technologies were incorporated in a weather model (the mesoscale weather research and forecasting coupled with a single-layer urban canopy model) at the city-scale. Our results showed that surface and rooftop heat mitigation strategies modify the meteorological fields and the dynamics of the lower atmosphere within the city during the hot summer days. The super-cool broadband radiative coolers are most proficient in decreasing ambient temperature and planetary boundary layer, followed by CMs, CC, GRs, and augmenting vegetation fraction. The super-cool broadband radiative coolers produced the most efficient strategy. Nevertheless, it has unintended consequences as they modify the temperature vertical profile, enhancing the stability over the urban domain and reducing the air's vertical mixing. The results presented show that the used model can be a valuable instrument to evaluate the implementation effects of heat mitigation

Key Points:

- Weather research and forecasting model is a valuable tool to evaluate the effects of heat mitigation measures in the urban environment for urban heat management
- Surface standard meteorological fields and lower atmospheric dynamics within the city are modified by heat mitigation measures
- The super-cool broadband radiative coolers yielded the most efficient strategy for urban cooling in tropical context

Supporting Information:

Supporting Information may be found in the online version of this article.

Correspondence to:

A. Khan,
khanansargeo@gmail.com

Citation:

Khan, A., Khorat, S., Doan, Q.-V., Khatun, R., Das, D., Hamdi, R., et al. (2023). Exploring the meteorological impacts of surface and rooftop heat mitigation strategies over a tropical city. *Journal of Geophysical Research: Atmospheres*, *128*, e2022JD038099. https://doi.org/10.1029/2022JD038099

Received 1 NOV 2022
Accepted 30 JAN 2023

Author Contributions:

Conceptualization: Ansar Khan
Funding acquisition: Dev Niyogi
Investigation: Rupali Khatun
Methodology: Ansar Khan, Mattheos Santamouris
Project Administration: Dev Niyogi
Software: Ansar Khan

© 2023. The Authors.
This is an open access article under the terms of the Creative Commons Attribution License, which permits use, distribution and reproduction in any medium, provided the original work is properly cited.

Supervision: Mattheos Santamouris, Dev Niyogi
Validation: Ansar Khan, Samiran Khorat
Visualization: Ansar Khan
Writing – original draft: Ansar Khan, Matei Georgescu
Writing – review & editing: Ansar Khan, Samiran Khorat, Quang-Van Doan, Rupali Khatun, Debashish Das, Rafiq Hamdi, Laura Carlosena, Matei Georgescu, Dev Niyogi

technologies in the urban environment for extreme urban heat management, such as the newly developed super-cool materials. However, careful attention should be paid to unintended consequences.

1. Introduction

The planetary boundary layer (PBL) is the lowest portion of the atmosphere and responds to surface forces, including frictional drag, evapotranspiration, heat and momentum transfer, and terrain-induced flow modifications, with a time scale of about an hour or less (Masson et al., 2020; Stull, 1988). The depth of the PBL varies spatially and temporally, ranging from hundreds of meters to a few kilometers. PBL depth can be measured as the height of potential temperature and mixing ratio inversions within the mixed layer or as the height where surface-driven turbulence production ceases (Brandi et al., 2021; Stull, 1988). PBL characteristics over urban areas are modified due to turbulent processes generated by the morphological structure of the urban fabric and anthropogenic heat (AH) release (Baklanov et al., 2011; Ching et al., 2019; Chow et al., 2012; Masson et al., 2020; Miao & Chen, 2008; Nadimpalli et al., 2022; Niyogi et al., 1999; Pelliccioni et al., 2016; Routray et al., 2010). During extreme heat events, the PBL structure is further altered via regulation of energy, and momentum, transport between the surface and overlying atmosphere, resulting in severe impacts on the health and quality of life of urban citizens (Hamdi et al., 2016, 2020; Patel et al., 2022; Tewari et al., 2023).

A range of heat mitigation technologies has been proposed to combat environmental consequences associated with extreme urban heat. These strategies fall under the broad umbrella of green infrastructure (e.g., urban lawns, trees, and green roofs (GRs)) and biophysical, or engineered, materials (e.g., cool materials (CMs)), including pavements and roofs, and super-cool broadband radiative coolers (Akbari et al., 2001; Baniassadi et al., 2019; Carlosena et al., 2020; Chow et al., 2012; Georgescu et al., 2013, 2014; Krayenhoff et al., 2018; Santamouris, 2014a, 2014b; Santamouris & Yun, 2020; Takebayashi & Moriyama, 2007). Broadband radiative coolers are emerging as a promising technology (Zhao et al., 2019), in large part because most heat mitigation technologies reduce daytime urban temperatures but have minimal impact during the evening and nighttime hours (Georgescu, 2015). Achieving daytime sub-ambient cooling has been a breakthrough in the field since buildings require cooling during the peak day period (Santamouris & Feng, 2018). To cool under the sun, materials need high reflectivity in the solar and high emissivity in the atmospheric window (8–13 μm). As a result, these materials have achieved more significant temperature reduction than CMs. A recent, low-cost scalable and sprayable polymeric materials reduced the baer substrates' temperature, under non-ideal climatic conditions with relative humidity up to 63%, up to 12°C temperature drops compared to the substrate (Carlosena et al., 2021). By maximizing the rejection of solar radiation and energy dissipation during all hours of the diurnal cycle, radiative cooling devices reach sub-ambient cooling under the direct sun without consuming additional energy while also reducing temperatures during nighttime hours (Z. Chen et al., 2016; Santamouris & Feng, 2018). A meta material film achieved a cooling power of 93 Wm^{-2} under direct sunshine at noon (Zhai et al., 2017). These types of materials have been studied recently on a city scale weather simulation models both during the summer and winter period. Researchers simulated the effect of three different super cool materials (SCMs) scenarios during the summer time in Kolkata metropolitan area (KMA) and found that the maximum decreases of net radiation varied between 468.3 and 236.3 Wm^{-2} and the maximum decreases of latent heat were between 41.3 and 13.1 Wm^{-2} (Feng et al., 2021). The SCMs are excellent urban heat mitigators, nevertheless they can lead to an overcooling penalty during the cold seasons. A study carried out in Kolkata concluded that under the most reflective and emissive scenario, the maximum decrease of net radiation was 354.9 Wm^{-2} (Khan, Khorat, et al., 2021).

Another study proposed different mitigation technologies on a street canyon and showed that radiative cooling materials were among the most efficient strategies in the study, decreasing up to 1.6°C ambient temperature and 24.2°C surface skin temperature (Bartesaghi-Koc et al., 2021). As mentioned before, CMs and SCMs are very reflective and can lead to an overcooling penalty at times. Recent research addressed this knowledge gap, calculating different solutions with optically modulated SCMs (Khan, Carlosena, et al., 2022). Optically modulated SCMs can be an efficient urban heat mitigation technology for use during the summer period without overcooling potential. Khan, Carlosena, et al. (2022) concluded that the modulation of both solar reflectivity and infrared emissivity could increase the ambient temperature up to 0.4°C and 1.4°C during the day and night, respectively. Decreasing the burden of heat for urban environments has considerable benefits across society, including reduction of energy consumption, improvement in thermal comfort and health (Akbari et al., 2004; Ali-Toudert et al., 2005; H. Chen et al., 2009; Santamouris, 2020; Santamouris et al., 2015).

Implementing urban heat mitigation technologies at the city-scale will modify surface heat and moisture transfer processes which will, in turn, modulate PBL dynamics. In general, higher sensible heat fluxes lead to more substantial vertical mixing over urban areas than rural surroundings. However, sensible heat flux is reduced due to the deployment of traditional heat mitigation strategies such as green and cool roofs, generating a less vigorous PBL with reduced vertical wind speeds and a lower PBL height (Brandi et al., 2021). For example, using the Weather Research and Forecasting (WRF) model, Sharma et al. (2016) reported a decrease in the PBL height of 0.5 km upon deployment of green/cool roofs across the Chicago Metropolitan Area. These results are consistent with Georgescu (2015), who demonstrated a reduction in turbulent kinetic energy and PBL height more significant for CMs than GRs under a scenario characterized by future urban expansion in California. Recent numerical modeling work has provided additional support indicating a decrease in primarily daytime PBL height with reduced impacts during non-sunlit portions of the diurnal cycle (Brandi et al., 2021; Song et al., 2018). However, much of the previous work has been conducted over cities located in developed nations (Yang et al., 2019). There is a need of similar research over conurbations in developing nations where meteorology, PBL dynamics, and human activities can lead to severe degradation of air quality. For example, Raman et al. (1990) reported that the PBL height of New Delhi (India) could reach 4.7 km during the pre-monsoon months. An important question is whether and to what extent would the deployment of heat mitigation strategies lower the height of the PBL, with important consequences for air quality (Charusombat et al., 2010) and health.

Additional modifications to urban environments (e.g., absorbed solar radiation via enhancement of reflective materials, relative humidity/water vapor via incorporation of green infrastructure, or wind speed and circulation) are likely to have a feedback that could compensate for the decrease in the PBL depth. For example, reduced ozone production can be expected if less solar radiation is absorbed because of cool roof deployment. Radiative coolers could increase the dryness of cities due to the offset of incoming solar radiation (i.e., less radiant energy available for partitioning to latent heat flux) and enhance the emission of longwave radiation. Incorporating green infrastructure may have unintended consequences on urban pollution, creating additional health problems (Santamouris & Osmond, 2020). Evidence is mounting that the built environment can modify convective precipitation (Hamdi et al., 2020; C. L. Zhang et al., 2009). Similar alterations in the surface energy balance, due to incorporating heat mitigation strategies, may further modulate precipitation magnitude or patterns over or downwind of urban areas (J. Liu & Niyogi, 2019).

We build upon previous work by focusing on the regional scale meteorological impacts of heat mitigation technologies on a tropical urban environment (Khan, Akbari, et al., 2022). A majority of urban heat mitigation studies for the tropics have focused on the application of different strategies to improve the thermal balance of large and medium-sized cities such as Singapore (Li & Norford, 2016; Mughal et al., 2019; Tan et al., 2015), Hong Kong (L. Chen & Ng, 2013; Cheng et al., 2010; Jim, 2015; Ng et al., 2012; Wong et al., 2013), Colombo (Emmanuel et al., 2007), Bhubaneswar (Swain et al., 2023), Mumbai (Dwivedi & Mohan, 2018), and Kolkata (Chatterjee et al., 2019). Despite the growing importance of urban climate mitigation research (Gonzalez et al., 2021; Khan, Akbari, et al., 2022; Krayenhoff et al., 2021), there exists a dearth of investigations focused on the impact of heat mitigation technologies on PBL dynamics in general and over tropical urban environments in particular. To our knowledge, there is no published assessment of the regional impact, in tropical urban areas, of the different presented heat mitigation strategies on lower atmospheric dynamics. The nexus between air pollution, green infrastructure, reflective materials, and human health remains unclear and requires examination prior to large-scale deployment.

This study aims to improve our understanding of the impacts of heat mitigation technologies on lower boundary layer dynamics at the city-scale using the WRF model. A historical and organically developed tropical coastal city characterized by a high-density residential area has been selected as our testbed: the (KMA). During the past decades, the KMA has undergone significant urban growth and has experienced considerable heat stress with continuously increasing urban heating intensity (Chatterjee et al., 2019; Khan, Akbari, et al., 2022). We build on prior work to investigate the potential impacts associated with the explicit representation of five different heat mitigation technologies. These include (a) cool materials - CMs, (b) super-cool broadband radiative coolers, (c) green roofs- GRs, (d) vegetation fraction change, and (e) a combination of these technologies. Our work addresses important environmental concerns associated with the city-scale deployment of urban heat mitigation

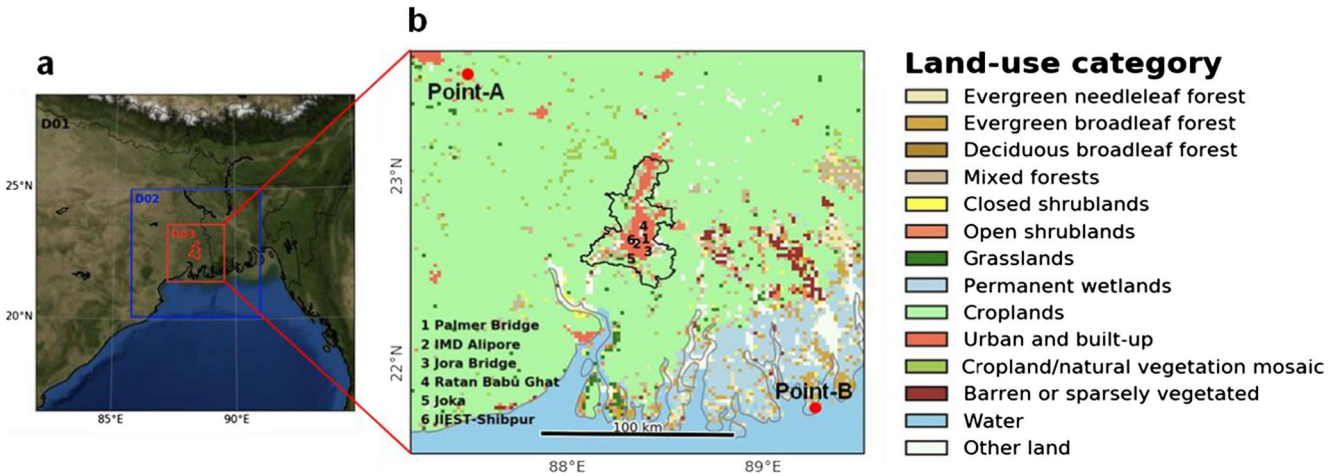

Figure 1. Weather Research and Forecasting domain shows (a) dynamical downscaling with domain 1 (d01) as outermost parent domain with 18 km grid spacing, domain 2 (d02) with 6 km grid spacing and, an (b) innermost domain (d03) with 2 km grid spacing encompasses the Kolkata metropolitan area. The Point-A (23°57′, 87°36) and Point-B (21°57′; 89°36′) are the points used for drawing horizontal-vertical cross-sections to analyze meteorological conditions for Figure 11. Six local meteorological observation stations were located by station codes for Palmer Bridge (PLB—1), Alipore (ALP—2), Jora Bridge (JRB—3), Ratanbabu Ghat (RBG—4), Joka (JKA—5), and Shibpur (SHP—6).

strategies for a large tropical city that normally receives scant research attention. Specifically, we ask the following research questions:

1. How effective are heat mitigation measures in the tropical urban environments?
2. How does a city-scale heat mitigation effort alter the city-scale thermal environment?
3. What is the spatio-temporal variability of the PBL dynamics caused by the heat mitigation measures?

2. Methods and Materials

To investigate the impact of different urban heat mitigation technologies on surface meteorological fields and PBL dynamics at city-scale, we employed the community Weather Research and Forecasting (WRF v4.3; Skamarock et al., 2021) model coupled with a single-layer urban canopy model (SLUCM, Kusaka et al., 2001). WRF is a state-of-the-art, non-hydrostatic, fully comprehensive mesoscale numerical weather prediction framework used here to investigate the effectiveness of implementing cool roof technologies on urban building's roof surfaces to mitigate the urban overheating and its influence on regional climate.

2.1. WRF Model Configuration

To address urban meteorological and environmental issues, SLUCM is dynamically coupled with the WRF Noah-Land Surface Model scheme (F. Chen et al., 2011). Our modeling domain utilizes three nested domains centered over KMA (22.57°N, 88.36°E) with a grid spacing of 18, 6, and 2 km (Figure 1). The details of the model physics parameterizations used in this study are listed in Table 1. The Kain-Fritsch (Kain, 2004; Zheng et al., 2016) convection scheme was used for the outer two domains but was turned off for the innermost domain. We used the default AH input in SLUCM with a fixed diurnal pattern, assuming a peak value of 50 and 90 Wm^{-2} for high-intensity residential and commercial areas.

We used the National Centers for Environmental Prediction (NCEP) Global Forecasting System operational global analysis and forecast data set (NCEP-GFS 0.25 Degree Global Forecast Grids, 2015) as initial and lateral boundary conditions during model integration. NCEP-GFS data are provided on a 0.25 × 0.25-° grid and are available at a three-hour frequency (https://rda.ucar.edu/datasets/ds084.1/). We focus our simulations on hot, pre-monsoon days characterized by considerable urban heating and associated health risk. Extreme heatwaves aggravate conditions in urban areas by boosting temperatures within the built environment and increasing urban temperatures more intensely than rural temperatures (Khan & Chatterjee, 2016; Khan, Akbari, et al., 2022). Under such adverse weather conditions, mitigation strategies are critically needed to reduce peak ambient temperatures and minimize any heat-related health risks. Therefore, we objectively selected sweltering days

Table 1
Weather Research and Forecasting Model-Coupled With Single-Layer Urban Canopy Model Configuration

Configuration	Domain 01 (D01)	Domain 02 (D02)	Domain 03 (D03)
Version		ARW-WRF Version 4.3	
Initial and boundary conditions		NCEP GFS 0.25º × 0.25º	
Run time		6 April 00:00 hr, 2020–8 April 00:00 hr, 2020 IST	
		6 April 00:00 hr, 2019–8 April 00:00 hr, 2019 IST	
		6 April 00:00 hr, 2018–8 April 00:00 hr, 2018 IST	
The period for analysis		7 April 00:00 hr, 2020–8 April 00:00 hr, 2020 IST	
		7 April 00:00 hr, 2019–8 April 00:00 hr, 2019 IST	
		7 April 00:00 hr, 2018–8 April 00:00 hr, 2018 IST	
Grid spacing (km)	18	6	2
Number of grid points in the x- and y-directions	75 × 75	91 × 91	121 × 121
Number of vertical layers		40 layers	
Microphysics		Purdue-Lin scheme Lin et al. (1983)	
Surface layer model		Noah-LSM + Single layer UCM Chen and Dudhia (2001), Kusaka et al. (2001)	
Turbulence		Mellor and Yamada's (1974) turbulent kinetic energy scheme	
Short-wave radiation		Dudhia (1989)	
Longwave radiation		Rapid radiative transfer model scheme Mlawer et al. (1997)	
Planetary boundary layer		Asymmetrical Convective Model version 2 (ACM2) Pleim (2007)	
Cumulus parameterization		Kain-Fritsch (KF) scheme Kain (2004) (only for outer two grids)	

with peak temperatures exceeding 39.2°C (Express News Service, 2021) for two consecutive very hot summer days during the pre-monsoon month of April to assess how heat mitigation strategies could impact the lower atmosphere of a tropical coastal city. We conducted 2-day simulations where the initial 24-hr is considered as model spin-up. This simulation is the control experiment compared to available observations to ensure model skill for appropriately reproducing the region's meteorology. In addition, we conducted sensitivity experiments (using an identical model configuration) to examine the impacts resulting from the implementation of a variety of heat mitigation strategies, including radiative coolers, cool roofs, GRs, increased vegetation fraction, and a final scenario that integrates the strategies above as a Cool city (CC) simulation (Table 2). The simulations were from 6 April through 8 April 2020, coinciding with India's critical COVID-19 confinement period (Khan, Khorat, et al., 2021). In addition, we have added two consecutive very hot summer days during the pre-monsoon month of April as additional case studies, each of 48-hr duration in the year 2019 and 2018. Further analysis were conducted with group of simulation that have different meteorological condition for each April month in the year 2019 and 2018 (Table 1). All WRF simulation output was analyzed for the concluding 24-h results. Our focus on simulation periods of a typical hot summer day, instead of the execution of the model in climate mode, permits the execution and analysis of a range of sensitivity tests to quantify the response of different heat mitigation technologies.

2.2. Numerical Design for Heat Mitigation Technologies

One base case (control) and five additional numerical simulations were carried out for the selected period for the present study. Initially, the control simulation with the original urban landscape (as represented by the moderate resolution imaging spectroradiometer data set) and urban parameter table were executed to assess the reliability of WRF by comparing simulation results with local observations. To better understand the regional influence of the different heat mitigation strategies on the urban environment, the Control case is considered the urban reference condition and is compared with simulations using different heat mitigation technologies. We simulated five types of heat mitigation technologies:

1. CMs, which increase the albedo value of all urban surfaces from 0.2 (control case) to a maximum of 0.65 (Morini et al., 2017);

Table 2
Numerical Design for the Regional Impact Study

Numerical design	Type of roof/surface	Mitigation strategies (high-density residential)		
		Albedo fraction	Emissivity fraction	Vegetation/Green fraction (rooftop/surface)
Control case	Conventional	Roof 0.20	Roof 0.90	–
		Wall 0.20	Wall 0.90	
		Ground (road) 0.20	Ground (road) 0.95	
Implemented heat mitigation cases				
Super-cool materials (SCMs)	Super-cool roof	Roof 0.96	0.97 for All	–
		Wall 0.20		
		Ground (road) 0.20		
Cool materials (CMs)	Cool roofs	Roof 0.65	Roof 0.90	–
		Wall 0.60	Wall 0.90	
		Ground (road) 0.45	Ground (road) 0.95	
Green roofs (GRs)	Green roofs	–	–	1.00 (rooftop)
Increased vegetation fraction (VEG)	Vegetative surface	–	–	0.50 (surface)
Cool city (CC)	Combined strategies	Roof 0.85	Roof 0.90	1.00 (rooftop)
		Wall 0.80	Wall 0.90	
		Ground (road) 0.65	Ground (road) 0.95	

2. GRs, which increase all roof covers to 100% green fraction and incorporate regular irrigation, ensuring soil saturation, at 20:00 local time. A total of 25 Lm^{-2} is set at the surface of the uppermost GRs layer (De Munck et al., 2018).
3. Vegetation fraction (VEG) increase, which reduced the urban fraction by 50%. We note that this is a realistic scenario that maximizes vacant spaces already available in the city (Chatterjee et al., 2019);
4. CC experiment, a combination of CMs and GRs (on building facets and surfaces, a higher increase in reflectivity and emissivity has been taken into consideration for these CMs) were simulated over the urban domain;
5. Super-cool materials (SCMs), which are more reflective than standard CMs, wherein the albedo and emissivity of all urban surfaces increased from 0.20 to 0.96 and 0.90 to 0.97, respectively (Feng et al., 2021).

Recent studies concern these newly developed SCMs. For example, a material based on titanium dioxide particles on top of silicon dioxide or silicon carbide nano particles with 90.7% solar reflectivity and a 90.11% sky window emissivity could theoretically achieve 5°C below ambient under direct solar radiation. However, the experiment conducted in Shanghai did not achieve sub-ambient cooling due to high humidity (Bao et al., 2017). On the other hand, a nano porous structure was tested in four different locations and climates. The material showed a distinct behavior in Phoenix, where it reached a sub-ambient temperature decrease of 3°C which is half of the cooling expected (Mandal et al., 2018). Moreover, a radiative cooler with 98% solar reflectivity showed a temperature decrease of up to 2.7°C at noontime under direct sunlight in humid Hong Kong and provided the proof of concept for the stringent solar reflectivity demand under high humidity (Zhong et al., 2020). Researchers have also calculated the cooling performance curve of an ideal emitter under different total water vapor columns. They found that the cooling power decreases from 115.9 to 32.6 Wm^{-2} with the increase of total water vapor from 0 to 6,000 atm-cm. However, subsequent increases in water vapor had a negligible effect, increasing from 6,000 to 8,000 atm-cm merely decreases by 3.3 Wm^{-2} (C. Liu et al., 2019). SCMs are extremely reflective when compared to third generation cool roofs or white paints, and are particularly effective at emitting radiation with wavelengths ranging from 8 to 13 μm (Santamouris & Yun, 2020). The field measurements have been carried out based on data from small samples tested over very short periods of time. These findings demonstrated that SCM cooling ability is influenced by the geography and climate of the city or location (Baniassadi et al., 2019; Feng et al., 2021). The cooling effect is more noticeable in dry atmospheres with a clear sky. However, when the atmosphere is cloudy or humid, available water vapor in the lower atmosphere may reduce the significant amount of infrared radiation emission (Lim, 2019). Our prior work for Kolkata (Feng et al., 2021) using SCM showed a good cooling potential despite the fact that Kolkata is a tropical wet and dry climatic city. As highlighted above,

Table 3
Comparison of the Simulation Results With Observation Data at 24-hr Scale

Parameters	ALP	RBG	SHP	PLB	JRB	JKA	Average
Correlation coefficient	0.97	0.98	0.98	0.98	0.98	0.98	0.98
Mean bias error	0.4	1.0	0.5	0.6	0.8	1.0	0.72
Mean absolute error	0.43	0.99	0.45	0.61	0.80	1.01	0.72
Root mean square error	1.2	1.9	1.2	1.7	1.4	1.4	1.5
Index of agreement	0.98	0.95	0.98	0.96	0.97	0.97	0.96

humidity plays a significant role in the ability of the materials to radiate heat. As the amount of water vapor in the atmosphere increases, the atmospheric transmittance decreases, and the atmospheric irradiance rises, causing the radiative cooler to absorb more atmospheric radiation and as a result, limit cooling performance. Although some experiments have not achieved sub-ambient temperatures under humid weather, others have shown considerable temperature reduction. Moreover, a few experiments have found that SCMs may not last in a variety of weather conditions or fit easily into all urban building environments (Gentle & Smith, 2015). Further details on the properties of each simulation are shown in Table 2.

3. Observational Data

We used six regional meteorological stations available from Weather Kolkata (http://www.weatherkolkata.in/, Indian Institute of Technology Kharagpur, 2020). Weather Kolkata provides in situ meteorological observations located within the urban boundary. These observational data are maintained by Kolkata Municipal Corporation. Of the six stations, three are urban stations (Palmer Bridge [PLB], Alipore [ALP], and Jora Bridge [JRB]) while the other three (Ratanbabu Ghat [RBG], Joka [JKA], and Shibpur [SHP]) are located in open spaces (academic institutes or parks) within high-intensity residential areas. The stations' locations and the innermost grid's boundary walls are shown in Figure 1. It is important to note that even though the present simulations represent a model configuration that accounts for 2 km grid spacing within the innermost grid, individual station readings are obtained at a particular spatial location. Therefore, we considered each station separately and compared the values of model-derived 2 m temperature and dew point temperature at the grid point nearest to the observation stations. In addition, the availability of observational data with a temporal frequency of 1-hr and equivalent model output generation allows for the assessment of the diurnal cycles. Besides this, we have also validated the PBL height with upper air Radiosonde data for variable energy cyclotron centre Calcutta Observations (Kolkata) (http://weather.uwyo.edu/) for city of Kolkata. The PBL height is not a direct observation and is estimated from sounding (only 1–2 times in a day) and ground-based data using Richardson approach (Lee & De Wekker, 2016; Schmid & Niyogi, 2012).

3.1. Model Evaluation and Validation

To evaluate the performance of the WRF-SLUCM system, we compared hourly simulated 2 m air temperature, dew point temperature, and upper air sounding against local measurements for the control case simulation over urban grid cells in the innermost domain. A statistical comparison of the mean bias error (MBE), mean absolute error, root mean square error (RMSE), correlation coefficient (r), and the index of agreement (IOA) for hourly 2 m air temperature for the 24-hr duration are listed in Table 3. The model evaluation is based on the correlation between the WRF simulations and observations for 2 m-temperature across the diurnal cycle (Figure 2). The coupled WRF-SLUCM model accurately captures the temperature observed at different stations (mean $R = 0.98$; mean bias = 0.72°C) for ALP, RBG, SHP, PLB, JRB, and JKA. The base case simulation produced urban meteorological conditions and statistically agreed with local observations ($p < 0.05$). The simulated average urban heat island (UHI) intensity varied from 1.8°C to 2.1°C for daytime and nighttime, respectively, in high-density residential areas relative to surrounding rural landscapes. The range of MBE and RMSE of air temperature was 0.4°C–1°C and 1.2°C–1.9°C, respectively. The range of IOA was 0.98 to 0.95, with average values of 0.96 when considering all observation stations. The model slightly underestimated the nighttime 2 m air temperature, potentially resulting from underestimating anthropogenic heating over the urban domain (Niyogi et al., 2020). We also assessed the impacts on local meteorological stations as they are most likely influenced when using the urban

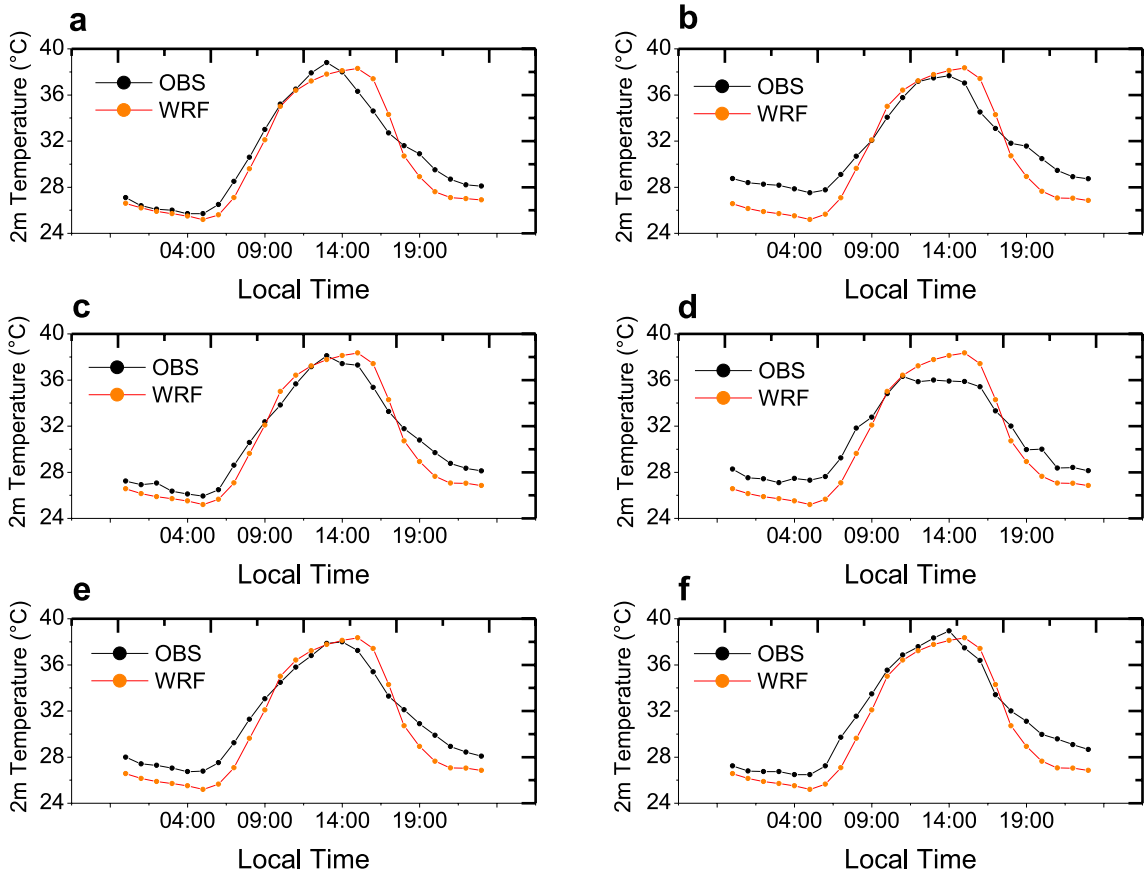

Figure 2. Validation of the Weather Research and Forecasting Model and the corresponding observed 2 m-temperature for six local meteorological stations (a) Alipore (ALP), (b) Ratanbabu Ghat (RBG), (c) Shibpur (SHP), (d) Palmer Bridge (PLB), (e) Jora Bridge (JRB), and, (f) Joka (JKA). The red and black circles are for the specific data in the high-density residential areas.

canopy scheme (UCM) scheme. The well-simulated daytime warming is balanced by the nighttime cooling, resulting in a diurnal range similar to observations. The threshold "comfort level" of dew points is greater than 20°C for the city stations. The difference is identical when quantifying impacts on local meteorological stations. Although WRF does not display considerable warm (comfort) bias over urban locales, the representation of the 24-hr averaged diurnal range of dew point temperature is well captured (Figure 3 and Table 4). In addition, model biases are most likely caused by: (a) lack of proper urban morphological representation and (b) uncertainties in model physical schemes, input data used, and locally meaningful urban biophysical parameters (Fung et al., 2022). Nevertheless, our initial evaluation highlights that the model can realistically replicate the urban environment, including a well-simulated evolution of the diurnal cycle of near-surface temperature and dew point. Moreover, the model framework can be used to examine regional meteorology and investigate the regional influence of different heat mitigation technologies.

The accurate representation of the PBL height is one of the important aspects for any sensitivity analysis, especially in simulation with turbulence, wind, and lower atmospheric impacts analysis. This is particularly important given our focus on lower atmospheric impacts. Our study uses a new combined local and nonlocal closure PBL scheme, the Asymmetrical Convective Model version 2 (ACM2) (Alapaty et al., 1997, 2001; Pleim, 2007). Overall, our results indicate a small overestimate in PBL height relative to observations (see Figure S1 in Supporting Information S1). The correlation coefficient of >0.85 for each year also indicates good agreement between simulated and observed PBL height. In particular, the model simulates the diurnal evolution of the PBL height well: the sharp ramp-up that occurs shortly after sunrise is reproduced accurately, as is the late afternoon/early evening collapse. Because PBL height is not a real observation, the performance of the WRF simulations is reasonable in terms of its ability to simulate high PBL height in tropical or sub-tropical atmosphere. A case study with ACM2 PBL scheme shows that the WRF model has performed reasonably well over the subtropical region of Delhi

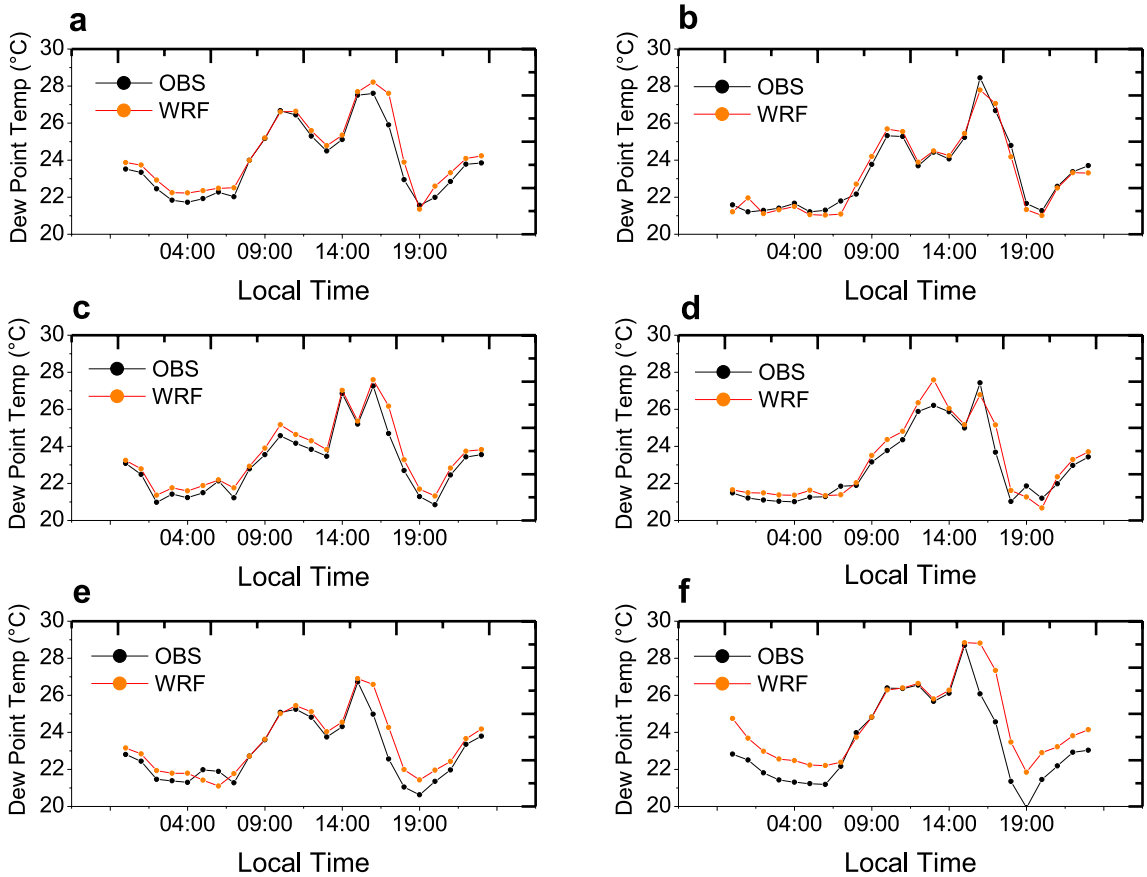

Figure 3. Validation of the Weather Research and Forecasting Model and the corresponding dew point temperature for six local meteorological stations (a) Alipore (ALP), (b) Ratanbabu Ghat (RBG), (c) Shibpur (SHP), (d) Palmer Bridge (PLB), (e) Jora Bridge (JRB), and, (f) Joka (JKA). The red and black circles are for the specific data in the high-density residential areas.

(Mohan & Bhati, 2011). The ACM2 PBL and Pleim surface layer scheme have been found to be well suited for short and extended simulations (i.e., few hour to more than a week) at the city-scale (Gilliam & Pleim, 2010).

4. Meteorological Impacts of Surface and Rooftop Heat Mitigation Strategies

In this section, we quantify the effect on near-surface meteorological impacts of the implementation of several heat mitigation technologies. The conventional roof is taken as the reference simulation for each urban configuration tested and summarized here for the year 2020 experiment.

Table 4
Observed and WRF-Simulated Mean, Maximum, Minimum, and Difference Between Maximum and Minimum dew Point Temperature Across the Six Local Meteorological Stations at 24-hr Scale[a]

	ALP		RBG		SHP		PLB		JRB		JKA	
Parameters (°C)	Obs	WRF	Obs	WRF	Obs	WRF	Obs	WRF	Obs	WRF	Obs	WRF
Mean	23.9	24.3 (+0.4)	23.2	23.2 (0.0)	23.1	23.5 (+0.4)	22.9	23.2 (+0.3)	22.9	23.3 (+0.4)	23.5	24.5 (+1.0)
Maximum	27.6	28.2	28.4	27.8	27.3	27.6	27.4	27.6	26.7	26.9	28.7	28.8
Minimum	21.6	21.4	21.2	21.0	20.8	21.3	21.0	20.7	20.6	21.1	19.9	21.8
Differences	6.0	6.9	7.2	6.8	6.4	6.3	6.4	6.9	6.1	5.8	8.8	7.0

[a]The number in parentheses denotes departure relative to observations.

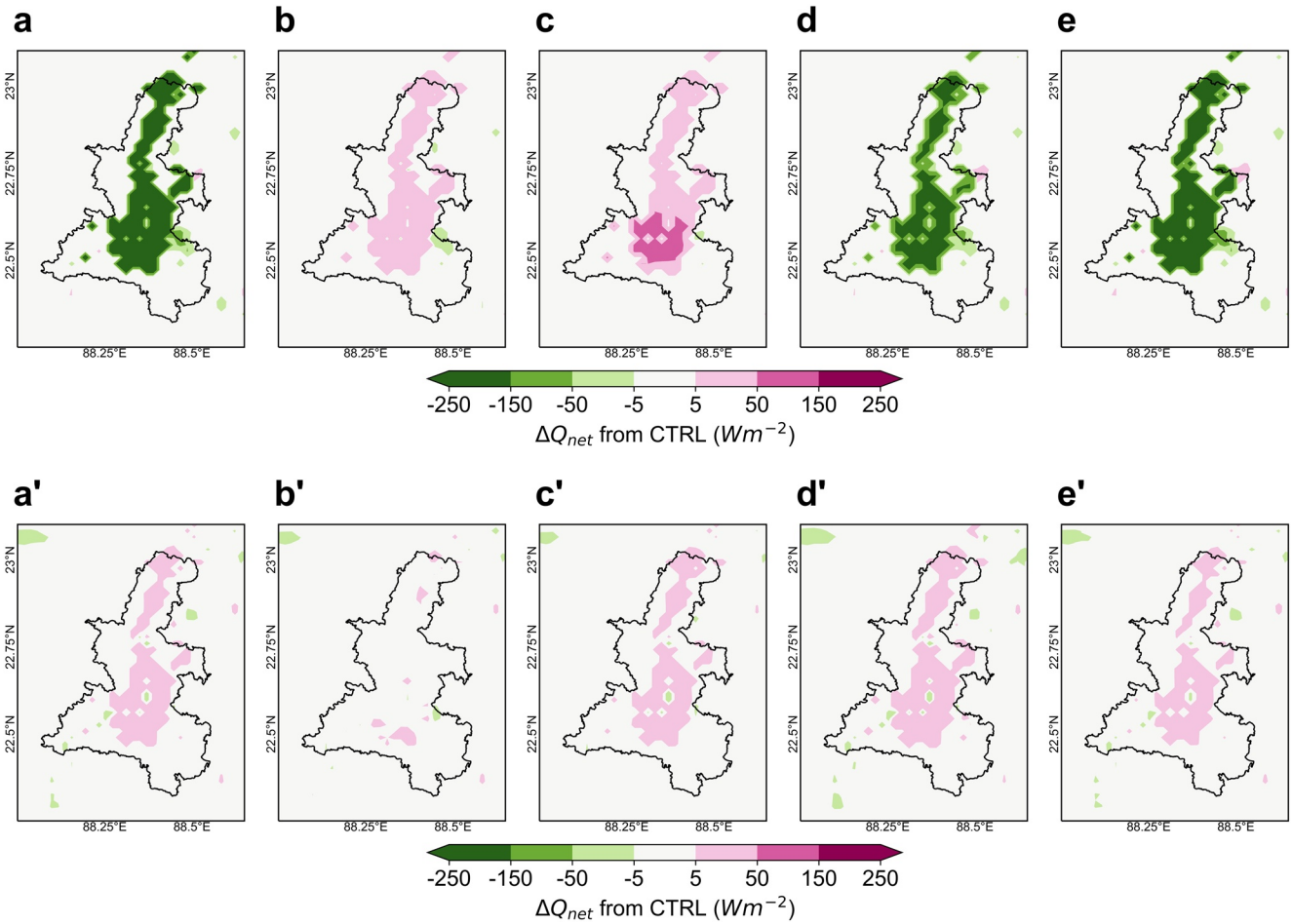

Figure 4. Changes (experiment minus control) in net inflow radiation during daytime (upper panel at 14:00 LT) and nighttime (lower panel at 2:00 LT) by different heat mitigations scenarios–(a-a') cool materials, (b-b') green roofs, (c-c') vegetation fraction changes, (d-d') cool city, and (e-e') super cool broadband materials over high-density residential building environments.

4.1. Regional Impacts on the Urban Energy Budget

The difference in the spatial variability of net radiation between the control case and sensitivity experiments incorporating different mitigation technologies (CMs, GRs, VEG, CC, and SCMs) is shown in Figure 4. The results, presented for daytime and nighttime conditions (14:00 LT and 02:00 LT), revealed that the maximum net radiative reduction was for SCMs and CMs due to their enhanced reflection of solar radiation. However, due to evaporative cooling over the urban domain, net radiation increased for GRs and VEG. The maximum decrease of sensible heat flux, at 14:00 LT, was 175.7 Wm^{-2} for CMs, 115.2 Wm^{-2} for GRs, 71.5 Wm^{-2} for VEG, 168.9 Wm^{-2} for CC, and 183.2 Wm^{-2} for SCMs (Table 5). The average decrease of sensible heat during the daytime was 100.1, 66, 42.2,96.8, and 101.8 Wm^{-2} for CMs, GRs, VEG, CC, and SCMs, respectively. On the other hand, during nighttime, impacts are reduced compared to daytime. The maximum reduction of latent heat flux over urban surfaces occurred at 14:00 LT and was 13.6 and 13.1 Wm^{-2} for CMs, and SCMs, respectively. Nevertheless, in the case of GRs, VEG, and CC scenarios, the latent heat flux simulated over urban surfaces at 14:00 LT increased by 163.5, 172.4, and 72.8 Wm^{-2}, respectively, compared to control. The diurnal profile of latent heat flux was also analyzed in this study. Simulations incorporating SCMs and CMs decreased the daytime latent heat flux by 7.6 and 7 Wm^{-2}, respec-

Table 5
Maximum Reduction of Heat Flux (Experiment Minus Control) by Different Heat Mitigation Technologies

Scenario	ΔQ_H (Wm^{-2})	ΔQ_L (Wm^{-2})	ΔQ_G (Wm^{-2})	ΔQ_{net} (Wm^{-2})
CMs	−175.7	−13.6	−84.8	−256.2
GRs	−115.2	163.5	−30.2	35.6
VEG	−71.5	172.5	90.6	41.8
CC	−168.9	72.8	−83.2	−162.2
SCMs	−183.2	−13.1	−58.6	−236.3

Note. ΔQ_{net} is the net inflow radiation to the surface, ΔQ_H is the sensible heat flux, ΔQ_L is the latent heat flux, and ΔQ_G is the heat flux into the ground.

Table 6
Changes of Heat Flux (Experiment Minus Control) by Different Heat Mitigation Technologies

	CMs	GRs	VEG	CC	SCMs
ΔQ_H (Wm^{-2})					
24-hr avg.	−60.7	−40.5	−33.3	−59.7	−60.9
Day	−100.1	−66.0	−42.2	−96.8	−101.8
Night	−15.8	−11.9	−22	−17.7	−13.3
ΔQ_L (Wm^{-2})					
24-hr avg.	−4.6	51.5	54.2	22.1	−4.1
Day	−7.6	94.7	109.4	41.3	−7.0
Night	−1.3	2.0	−1.0	−0.08	−1.0
ΔQ_G (Wm^{-2})					
24-hr avg.	9.0	−2.8	4.3	6.6	−6.6
Day	35.5	6.8	37.8	32.6	23.1
Night	−24.0	−15.0	−29.3	−25.9	−19.6
ΔQ_{net} (Wm^{-2})					
24-hr avg.	−74.3	13.8	16.6	−44.2	−69
Day	−143.2	21.9	26.9	−88.1	−132
Night	6.9	5.1	6.3	8.1	5.6

tively, and increased the latent heat for GRs, VEG, and CC by 94.7, 109.4, and 41.3 Wm^{-2}, respectively (Table 6). We note that our analysis of mitigation technologies' effect on surface energy fluxes was performed without first evaluating whether the model could successfully replicate the surface energy balance. Models that simulate the 2-m air temperature well, do not necessarily correctly simulate the surface energy balance (Shaffer et al., 2015). In the absence of available surface energy balance data, as they do not exist for the locations and period of investigation, we compared our control simulation results with values from the literature. Therefore, we used the reported heat flux results from Singapore, a tropical city that has been the focus of considerable research, as a reference. Results revealed a maximum decrease of sensible heat flux at 14:00 LT of 180 Wm^{-2} when highly reflective materials were applied on building rooftops and a maximum decrease of sensible heat flux of about 85 Wm^{-2} when the green vegetation fraction in the urban landscape was increased.

The surface energy balance for urban areas resulting from the deployment of various heat mitigation technologies in different tropical cities is also presented. For example, Li and Norford (2016) reported that the maximum decrease of latent heat flux at 14:00 LT was about 20 Wm^{-2} for CM technologies, but a latent heat flux increase of 195 Wm^{-2} was simulated by increasing green vegetation cover for Singapore. These reported values are similar to the present results for the tropical context.

The maximum decrease of heat storage occurred at 14:00 LT, and the values were 84.8, 90.8, 90.6, 83.2, and 58.6 Wm^{-2} for CMs, GRs, VEG, CC, and SCMs, respectively. The maximum reduction of net inflow radiation during peak hour (14:00 LT) was 256.2, 162.2, and 236.3 Wm^{-2} for CMs, CC, and SCMs respectively, but an increase of Q_{net} during the peak hour (14:00 LT) was found in GRs and VEG of 35.6 and 41.8 Wm^{-2}, respectively. These result from the high temperature at mid-afternoon, low surface albedo (conventional reflective surfaces), and warmer lower atmosphere than the ground surface. The average decrease of Q_{net} over the urban surface during daytime was 143.2, 88.1, and 132 Wm^{-2} for CMs, CC, and SCMs, respectively, but an increase in Q_{net} of 21.9 and 26.9 Wm^{-2} for GRs and VEG was found. On the other hand, during nighttime, the average increase of Q_{net} was 6.9, 5.1, 6.3, 8.1, and 5.6 Wm^{-2} for CMs, GRs, VEG, CC, and SCMs, respectively. The changes in the surface energy budget directly impact near-surface variables and the overlying PBL, which are the focus of the subsequent sections.

4.2. Regional Impact on Surface Meteorological Fields

In this study, we used 2 m ambient air temperature ($\Delta T_{ambient}$), surface skin temperature ($\Delta T_{surface}$), 2 m dew point temperature (ΔT_{dew}), relative humidity at 2 m ($\Delta H_{relative}$), and 10 m-wind speed (ΔW_{speed}) to examine the regional impact of different heat mitigation technologies. The difference of 2 m ambient air temperature ($\Delta T_{ambient}$) between the control and experimental cases showed that the SCM simulation exerted the largest regional influence for most experiments. The GRs experiment led to a decrease in $\Delta T_{ambient}$ of 0.88°C, as a result of rooftop gardening transpiration. Results showed that the maximum reduction of $\Delta T_{ambient}$, over urban areas, at 14:00 LT was1.6°C for SCMs, 1.5°C for both CMs and VEG, and 1.4°C for the CC experiment (Table 7). The diurnal profile of $\Delta T_{ambient}$ reduction is also presented as average over daytime and nighttime for each experiment (Figure 5). During the daytime, the average $\Delta T_{ambient}$ decreased by 1.1°C for SCMs, 0.7°C for GRs, 0.5°C for VEG, and 1.1°C for CMs and CC. The average $\Delta T_{ambient}$ for CMs and CC were spatially distributed over the urban surface.

On the other hand, during nighttime, the thermal reduction was less compared to daytime: 0.6°C, 0.59°C, 0.67°C and 0.4°C for SCMs, CMs, CC, and GRs, respectively. The nighttime reduction for SCMs occurred because of the high emissivity value of 0.97. When the vegetation fraction over urban areas increased, the thermal reduction of $\Delta T_{ambient}$ during nighttime was greater (by 0.8°C) than daytime due to the regular supply of sufficient moisture (at 20:00 local time) for GRs with irrigated surface and less storage during the day. Different heat mitigation technologies resulted in a decrease of urban $\Delta T_{surface}$ during daytime and nighttime. This decrease resulted from the offset of incoming solar radiation and the effects of green infrastructures whose residual impacts lasted into

Table 7
Reduction (Experiment Minus Control) of 2 m Ambient Temperature $\Delta T_{ambient}$ (°C) and Surface Skin Temperature $\Delta T_{surface}$ (°C) Over Urban Area

	$\Delta T_{ambient}$ (°C)			$\Delta T_{surface}$ (°C)		
Scenario	Maximum decrease	Daytime average (05:00–17:00)	Nighttime average (18:00–04:00)	Maximum decrease	Daytime average (05:00–17:00)	Nighttime average (18:00–04:00)
CMs	−1.5	−1.1	−0.59	−4.0	−2.8	−0.9
GRs	−0.88	−0.7	−0.4	−2.5	−1.7	−0.6
VEG	−1.5	−0.5	−0.8	−2.3	−1.3	−1.2
CC	−1.4	−1.1	−0.67	−4.0	−2.7	−0.9
SCMs	−1.6	−1.1	−0.6	−4.2	−2.9	−0.7

Note. The values are separated into 24-hr average, the daytime and the nighttime.

the evening and nighttime hours (Figure 6). Results indicate that the SCM experiment resulted in the greatest maximum reduction of $\Delta T_{surface,}$ 4.2°C, primarily due to the high reflectivity value used in walls and ground; as a result, it had the highest regional impact among the strategies discussed. The average ambient temperature decrease caused by heat convention was substantially higher in the low density than in the high-density parts of the city. The CMs and CC experiment revealed a decrease of $\Delta T_{surface}$ by 4°C for both experiments. The average

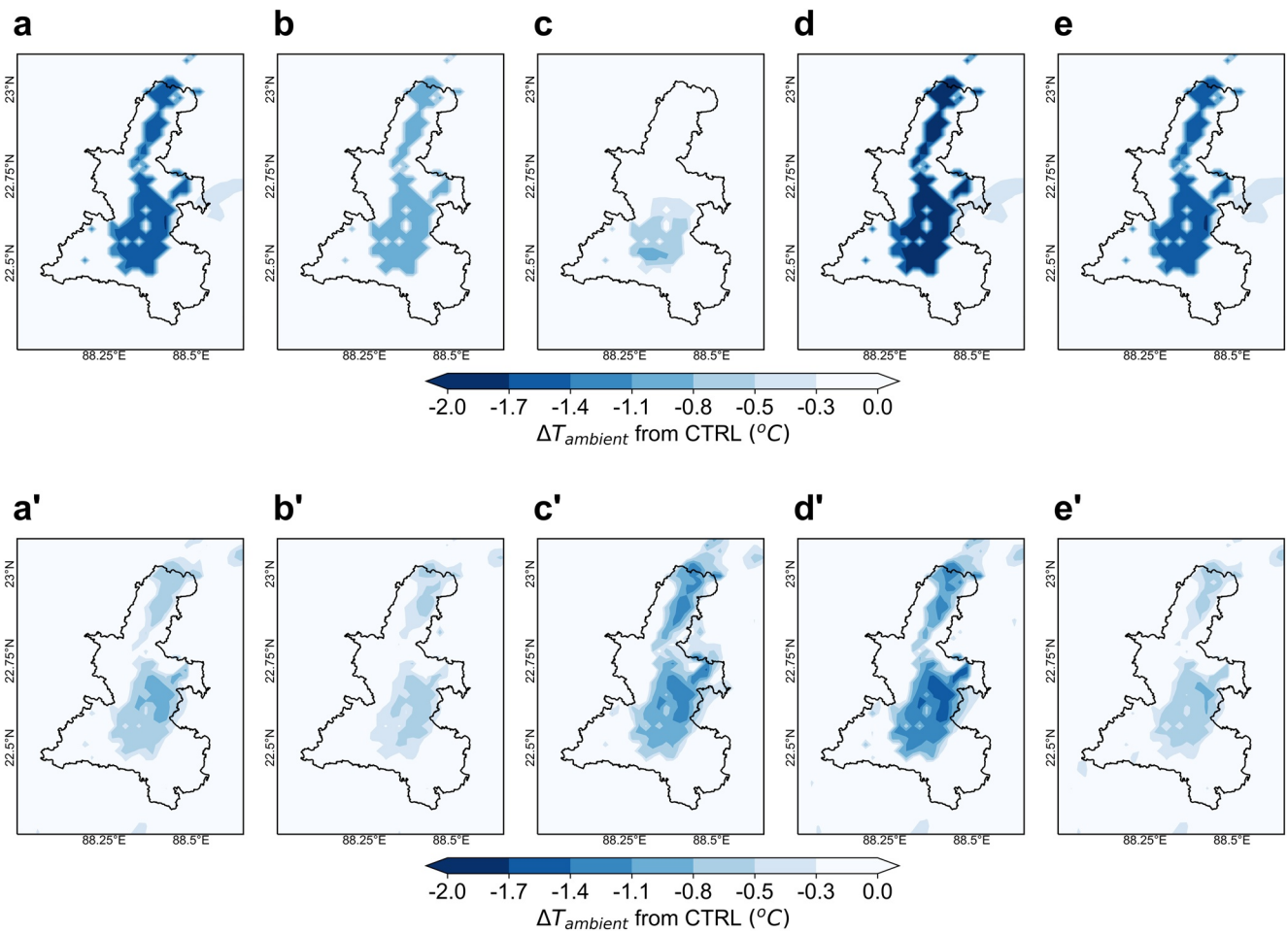

Figure 5. Changes (experiment minus control) in 2 m ambient temperature during daytime (upper panels at 14:00 LT) and nighttime (lower panel at 2:00 LT) by different mitigation scenarios-(a-a') cool materials, (b-b') green roofs, (c-c') vegetation fraction changes, (d-d') cool city, and (e-e') super cool broadband materials over high-density residential building environments.

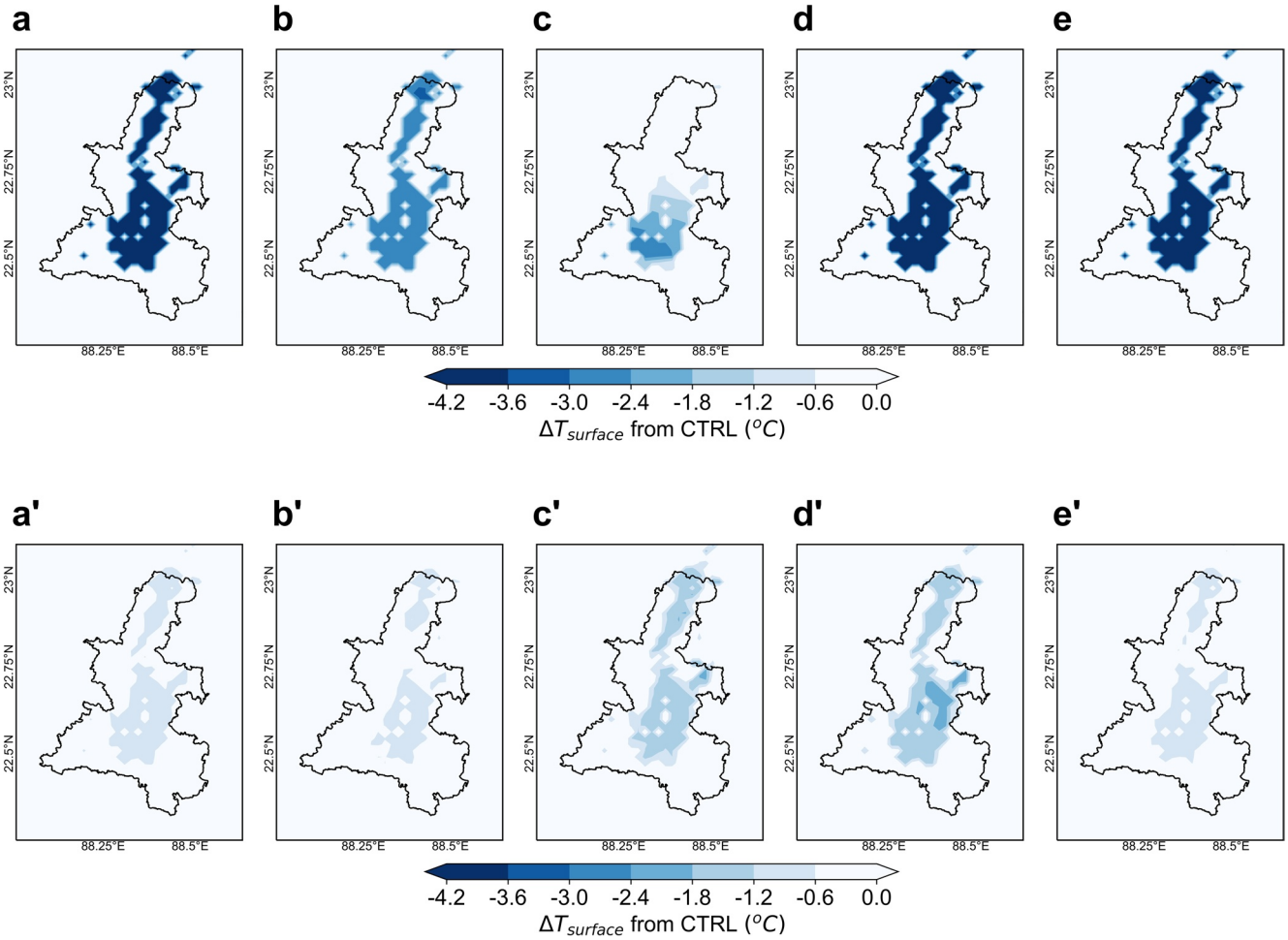

Figure 6. Changes (experiment minus control) in surface air temperature during daytime (upper panel at 14:00 LT) and nighttime (lower panel at 2:00 LT) by diffent heat mitigation scenarios- (a-a') cool materials, (b-b') green roofs, (c-c') vegetation fraction changes, (d-d') cool city, and (e-e') super cool broadband materials over high-density residential building environments.

reduction of $\Delta T_{surface}$ during the daytime was 2.9°C for SCMs, 2.8°C for CMs, 2.7°C for CC, 1.7°C for GRs, and 1.3°C for VEG. The increase of moisture content resulting from additional evapotranspiration with the use of GRs and increasing vegetation fraction (VEG) led to an increase of ΔT_{dew} of 2.5°C for GRs, VEG, and combined cases; the changes in near-surface ΔT_{dew} were negligible in the CMs and SCMs experiment but during nighttime ΔT_{dew} underwent a slight increase over urban areas (Figure 7). In the case of the SCMs experiment, near-surface ΔT_{dew} endured maximum increase of 2.1°C due to the presence of high humidity. By impacting $\Delta T_{ambient}$, a modification of near-surface relative humidity was simulated for all thermal mitigation strategies (Figure 8).

The SCMs experiment showed a robust regional effect on $\Delta H_{relative}$ (a maximum decrease of more than 3% compared to the control case). Compared to the control case, the increase of $\Delta H_{relative}$ during daytime was slightly less than 2.5% for both CMs and GRs. Nevertheless, the VEG and CC experiment increases by 2.5%–3.5% over the urban core area because of additional evapotranspiration. Wind speed also changed by implementing different heat mitigation technologies over the urban area. The SCMs experiment showed a maximum change of wind speed (an increase of 2 ms^{-1}) over the urban domain during the daytime due to a modification of surface absorbed solar radiation, which affects the local surface pressure variability that gives rise to microscale circulation. The GRs experiment did not considerably affect the wind speed, further influencing the ambient temperature reduction. Nevertheless, the CMs and CC slightly increased wind speed during the daytime due to the thermal gradient between core-urban to suburban environments. In tropical warm climates elevated roof surface skin temperatures caused by the absorption of solar radiation are undesirable. Reflective surface coatings aid achievement of high solar reflectance. This might notably cool the urban environment by reflecting infrared rays.

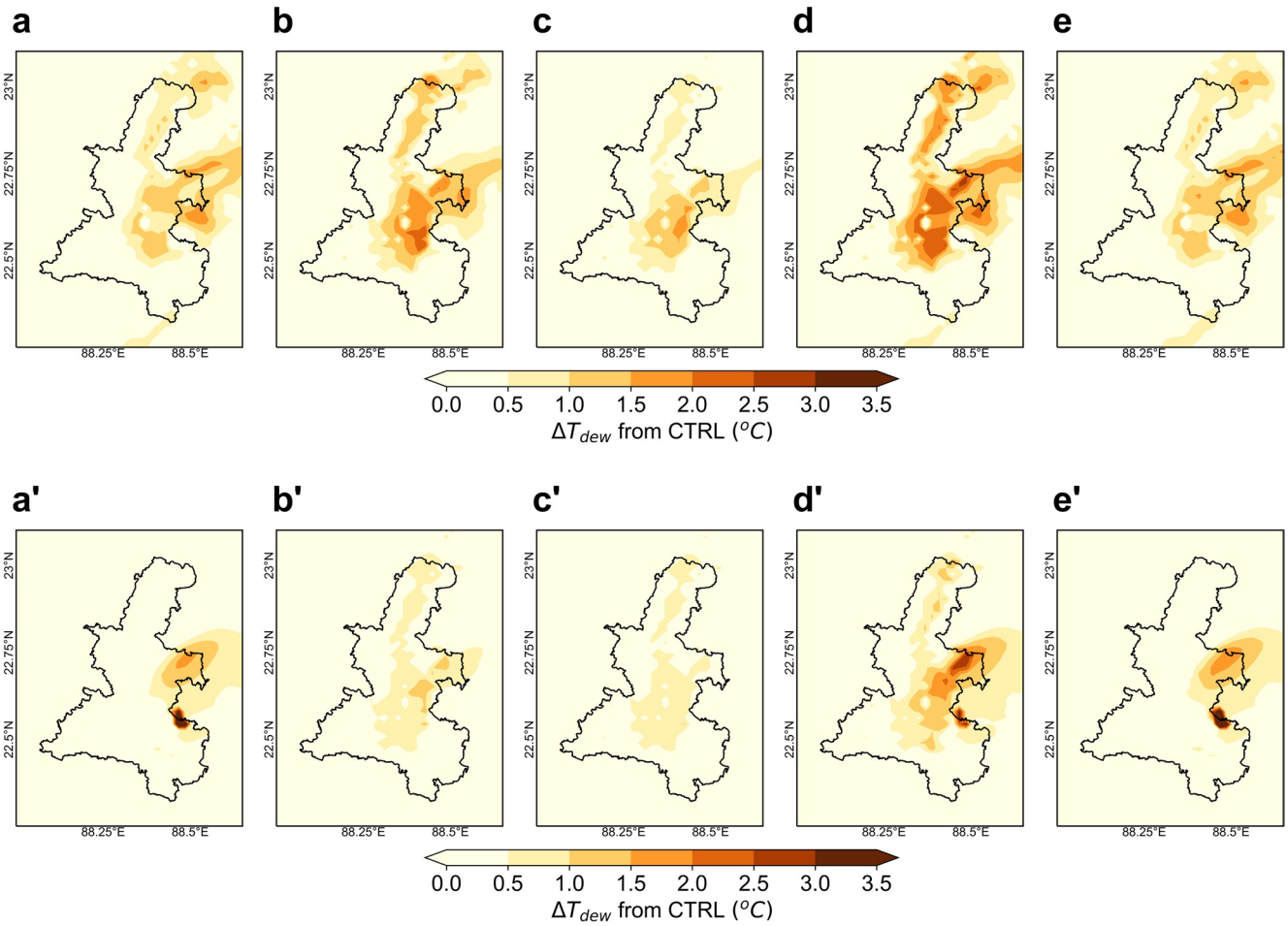

Figure 7. Changes (experiment minus control) in dew point temperature at 2 m height during daytime (upper panel at 14:00 LT) and nighttime (lower panel at 2:00 LT) by different heat mitigation scenarios (a-a') cool materials, (b-b') green roofs, (c-c') vegetation fraction changes, (d-d') cool city, and (e-e') super cool broadband materials over high-density residential building environments.

The implementation of heat mitigation technologies certainly changes the urban radiative and non radiative properties. The uses of different heat mitigation strategies reduce the sensible heat available for transmission to the air or to building envelopes. The CCs (combined of CM and vegetation) increases the evapotranspiration in urban areas through soil and plants on surface (redirecting available energy to latent heat), while a reflective material increases the reflection of incoming solar radiation in urban areas by increasing the albedo of roof surfaces. These mechanisms can be further illustrated by considering the one-dimensional energy balance for an infinitesimally thin layer of roof materials at the roof-air interface by simple urban energy balance. The SCMs, CMs, and CCs impact on the wind speed differ due to higher reflectivity of the materials and vegetation effects. Results show that the maximum urban heating is reduced during the peak hour for all experiments. SCMs are more efficient than the CMs and CCs in reducing the urban heating with maximum differences due to "regional high" effects. The reductions of the urban heating vary linearly with the increasing materials fractions, but slightly nonlinearly with the increasing albedo for few hours. The maximum reduction in wind speed is simulated with SCMs, and CMs. While previous studies report that the advection of moist air from rural areas is a key mechanism, this study shows that this is not the case for the extreme urban event due to the very dry and warm conditions, and instead, convective rolls could play a more important role (Niyogi et al., 2006).

4.3. Regional Impacts on Atmospheric Boundary Layer Dynamics

The different mitigation technologies of urban heating can change the near-surface meteorological condition and modify the atmospheric boundary layer structure (Mills et al., 2022; Niyogi et al., 2011; A. Sharma et al., 2016).

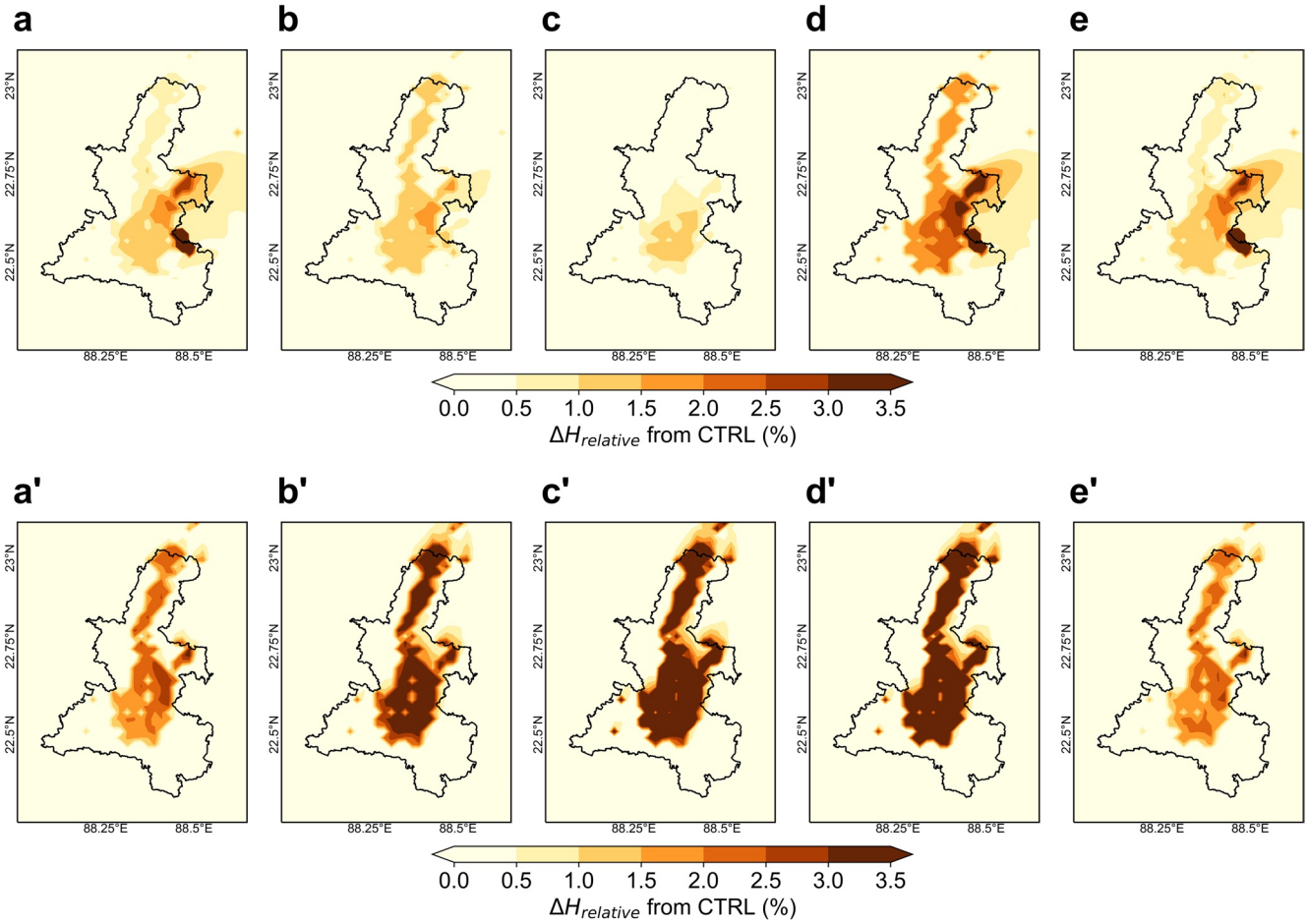

Figure 8. Changes (experiment minus control) in relative humidity at 2 m height during daytime (upper panel at 14:00 LT) and nighttime (lower panel at 2:00 LT) by different heat mitigation scenarios- (a-a') cool materials, (b-b') green roofs, (c-c') vegetation fraction changes, (d-d') cool city, and (e-e') super cool broadband materials over high-density residential building environments.

Our simulation results showed that all the thermal mitigation experiments would modify the atmospheric boundary layer structure over the urban area, although this impact was apparent mainly during the daytime (Figure 9). Some comparatively small changes also occurred outside the urban areas. These results might be numerical artifacts resulting from numerical instabilities of the model rather than the surface-induced forcing that was illustrated for KMA. In general, the atmospheric boundary layer structure dynamics are strongly regulated by the heating at the surface, which manifests as changes in the PBL state (Song & Wang, 2015; D. L. Zhang et al., 2011).

The simulated vertical profile of temperature, relative humidity, and wind speed over the urban environment was used to investigate the impact of the atmospheric boundary layer structure. The maximum reduction of the air temperature of the cool roof and CC experiment extended from the urban surface to approximately 0.3 km at night, and a gradual decrease of air temperature up to 2.5 km occurred at 14:00 LT (Figure 10). Heat mitigation strategies are expected to augment the static stability of PBL at a diurnal scale and reduce the magnitude of vertical winds, enhancing subsidence in the lower atmosphere (Brandi et al., 2021). The maximum decrease of air temperature occurred during the daytime, extending from the urban surface to approximately 2 km in the PBL. For the GRs experiment, the maximum reduction of air temperature extended from the urban surface to approximately 0.5 km above, at noon, of the simulated period. The SCMs simulation led to a maximum decrease of vertical air temperature over urban surfaces, with an impact extending to 1.5 km during daytime. Above the atmospheric boundary layer, the rate of reduction of air temperature gradually decreased compared to the atmospheric boundary layer below. During the daytime, an increase of relative humidity (greater than 9%) was evident within the atmospheric boundary layer, but a decrease of similar magnitude was found above the

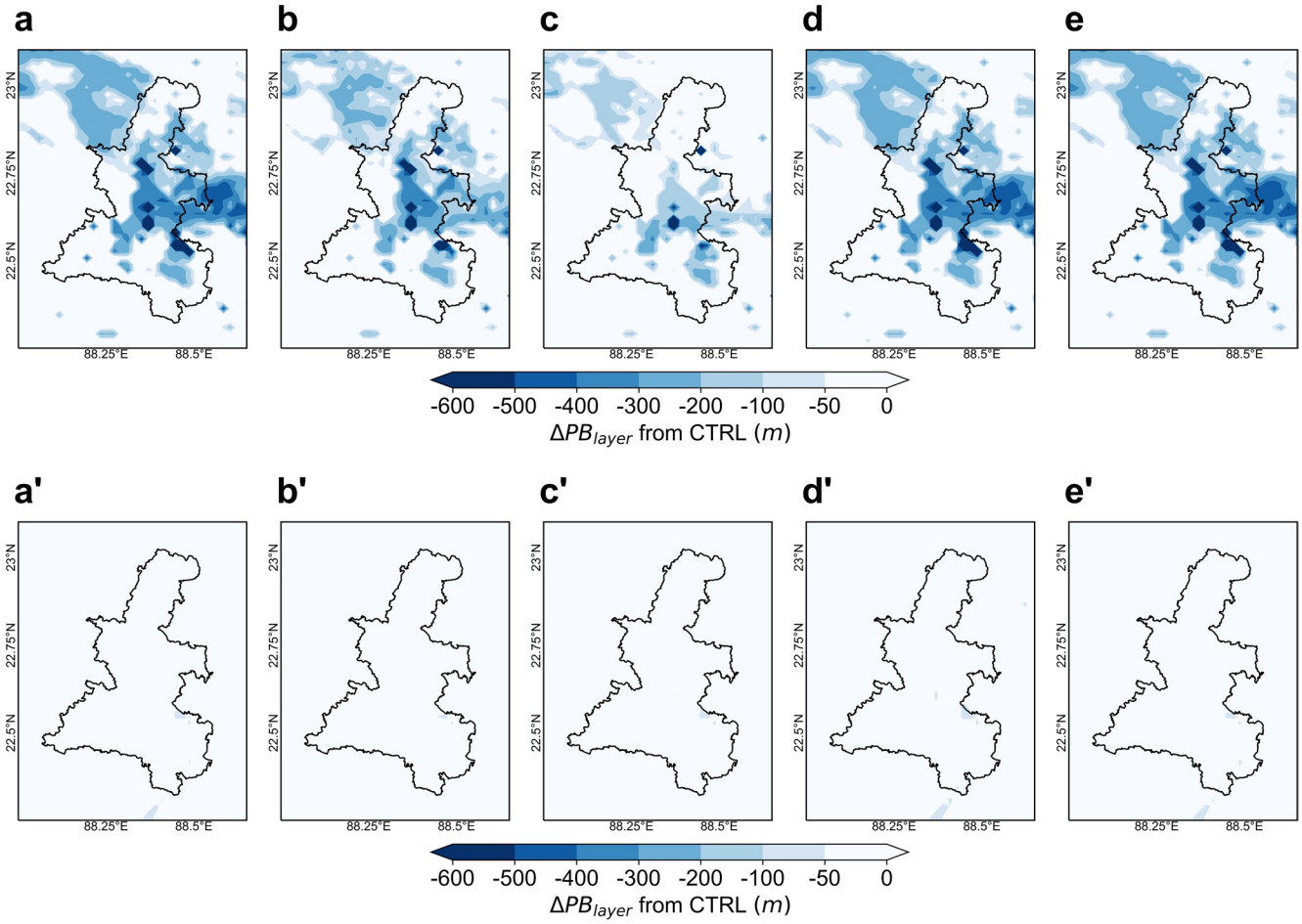

Figure 9. Changes (experiment minus control) in planetary boundary layer height during daytime (upper panel at 14:00 LT) and nighttime (lower panel at 2:00 LT) by different heat mitigation scenarios (a-a') cool materials, (b-b') green roofs, (c-c') vegetation fraction changes, (d-d') cool city, and (e-e') super cool broadband materials over high-density residential building environments.

boundary layer. In the GR experiment, relative humidity changes were less significant than the other daytime scenarios. The maximum increase of relative humidity occurred during daytime hours and extended up to 1 km from the urban surface in the SCMs experiment. The vertical wind speeds decreased during daytime and slightly increased during nighttime, extending from the urban surface to approximately 3.5 km for all experiments. The maximum decrease of vertical wind speed that occurred during daytime was 0.5 ms^{-1} in the SCMs experiment due to a deficit in input solar radiation. We found that daytime PBL height significantly decreased over the urban area by 600 m for SCMs and 500 m for CMs and CC experiments, but the GRs and VEG experiment underwent reduced modification of the PBL over the urban area. On the other hand, the PBL height underwent an increase for both CMs and GRs during nighttime.

4.4. Regional Impact on Sea Breeze Circulations

The impact of land surface heterogeneity with large-scale implementation of heat mitigation strategies on sea breeze circulation of an urban area in a tropical environment has become an important subject of scientific interest (Bechtel et al., 2017; Chatterjee et al., 2019; Patel et al., 2020). The intensification of sea breeze circulation is dependent on the large-scale synoptic background, which plays an essential role in modulating the prevailing wind near the surface (Freitas et al., 2007). This local circulation occurs due to a thermal incongruity between land and sea (Lin et al., 2008; Wang et al., 2018). There is mounting evidence that these circulations can extend more than 100 km horizontally inland (Hamdi et al., 2012), and vertically may reach up to 3 km during mid-afternoon. In the vertical dimension, the height of the PBL in tropical coastal cities is associated closely with

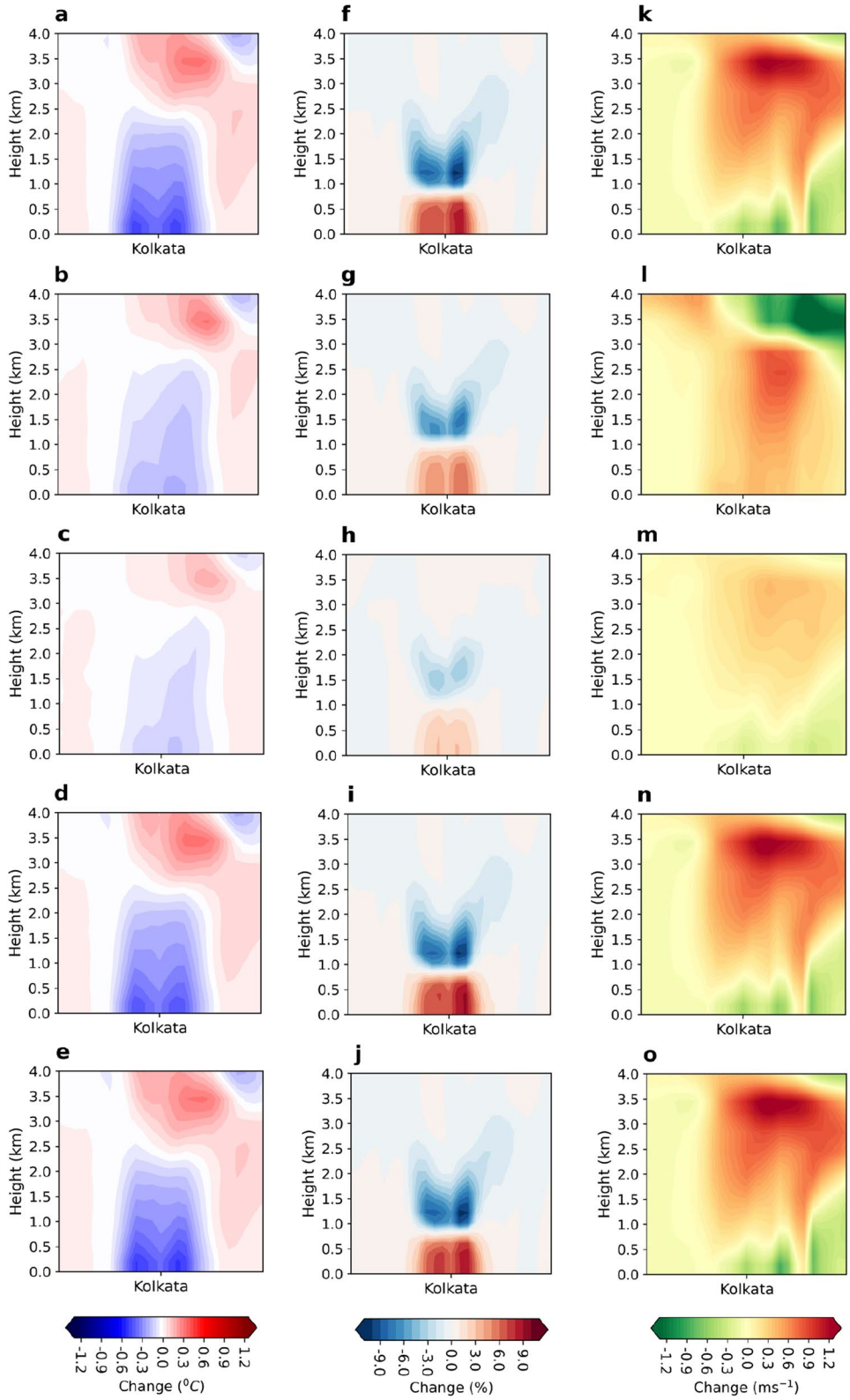

Figure 10. Vertical distribution profile of standard meteorological fields for the different heat mitigations impact during peak hour (14:00 LT) over Kolkata (north-south)–(a-f-k) cool materials, (b-g-i) green roofs, (c-h-m) vegetation fraction change; (d-i-n) cool city model, and (e-j-o) super-cool broadband materials. For (a-e, f-j, and k-o) represent the changes in air temperature, relative humidity, and wind speed, respectively.

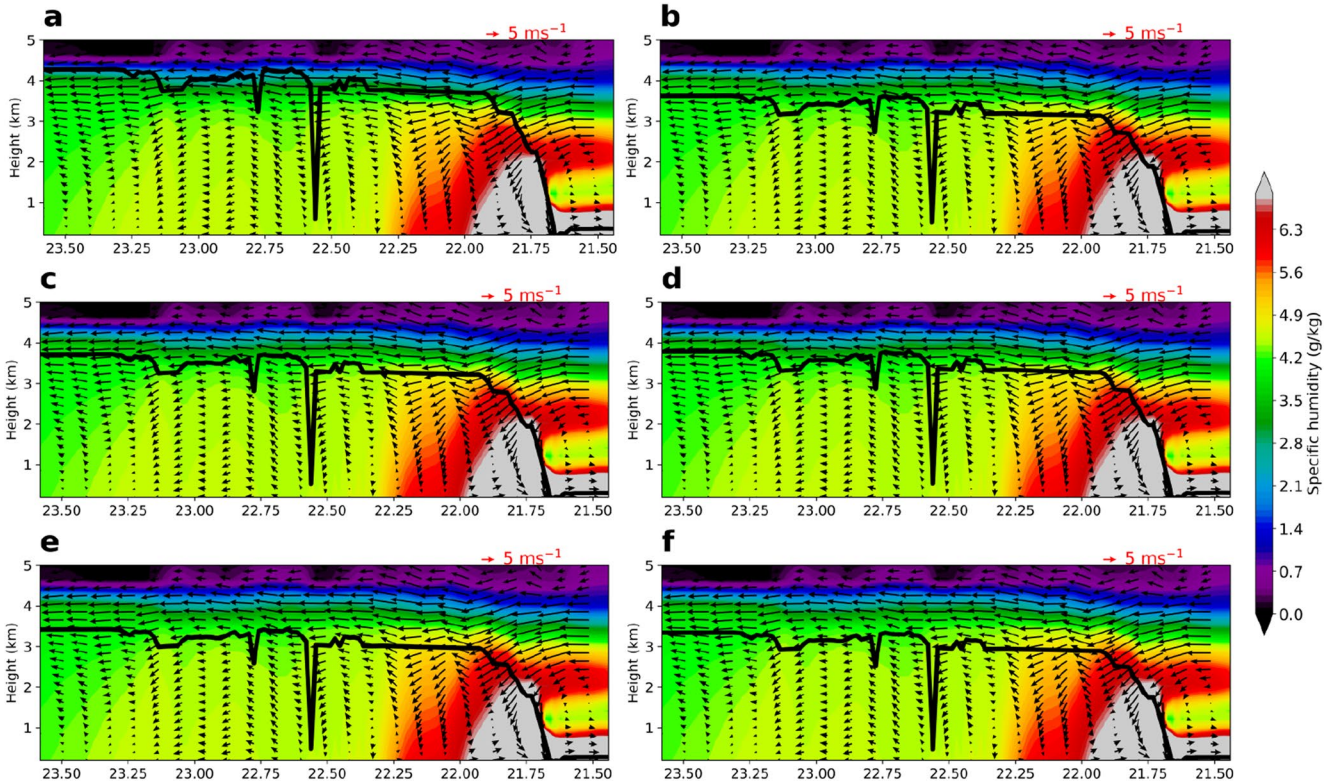

Figure 11. Cross-sectional profile of different heat mitigations impacts on sea breeze during peak hour (14:00 LT) over Kolkata (see Figure 1's Point-A and Point-B) (a) control case, (b) cool materials (CMs), (c) green roofs, (d) vegetation fraction change; (e) Cool city (CC) model, and (f) super-cool broadband materials. The vertical gradient of specific humidity determines the static stability of the lower atmosphere. For high solar radiation, the convective boundary layer developed fast way and progressively decreased with implement of (b) CMs, (e) CC model, and (f) super cool broadband materials. The planetary boundary layer (PBL) is lower over the city center and adjoining water surface. The larger drop in PBL is due to heat mitigation effects in densely packed urban areas of the city. Due to super-cool broadband materials, the PBL (black thick line) tends to be much lower due to offset of direct solar energy and reduced the vertical wind speeds during daylight. This effect, in turn, led to lower vertical convective mixing. The PBL also rapidly contracts due to a reduction of thermals from the urban surface after sunset and low temperature. The thermal characteristics of the surface, influence the diurnal range of surface skin temperatures, and net inflow radiation at the surface and its variation with height, which determine the radiative warming or cooling of the surface and the PBL associated with heat mitigation options.

the advection of the sea breeze. The circulation can be modified when a heat mitigation strategy is implemented. The heat mitigation strategies could alter the PBL height and potentially trigger localized circulation over the urban domain.

Our results indicated that the onset of the sea breeze was delayed to mid-afternoon due to the "regional high" effect within the lower PBL and offshore synoptic wind above the PBL (Niyogi et al., 2020). The denser cool air over the urban domain flowed toward the suburban area to replenish the buoyant warm air due to urban cooling by city-wide implemented heat mitigations technology or strategies. The CMs and SCMs could suppress the vertical lifting of urban thermals, modifying low-level motions in hot summer days resulting in a deceleration of the sea breeze front compared to other strategies. In some cases, the cooling effects of sea breezes appeared to be more discreetly in the urban center due to surrounding high-rise buildings and their roughness parameters (Figure 11). The sea breeze-based cooling was not directly transferred to the surface due to surface roughness heterogeneity and internal boundary layers (Gilliam et al., 2004). The horizontal wind shear and frontal lifting owing to surface roughness and heterogeneity could setback the onset of sea breeze front in the urban core. The potency of the sea breeze advection was subjected to the dimension of the city, which moderates the urban heating effect. Thus, our results indicate that urban heat mitigation strategies have modified the thermal and dynamic profile in the urban boundary layer and sea breeze circulation (Aflaki et al., 2017; Niyogi et al., 2020; Wang et al., 2018). This synoptic flow prevailed in the opposite direction of sea breeze, and a weakened sea breeze development can lead to the accumulation of secondary pollutants in the back of the front. As shown in Patel et al. (2021), there is also likelihood that a convergence band can be formed due to green roofing, which can create localized heavy rains.

We also found changes in the moisture fields for our thermal case, which could potentially trigger afternoon thunderstorms.

5. Sensitivity Analysis for Different Meteorological Conditions

We conducted one control, in addition to a five-sensitivity experiment for consecutive 3 days (of 2018, 2019, and 2020) during pre-monsoon seasons. In 2020, we conducted a 2-day simulation where an initial 24-hr is considered as model spin-up time and remaining 1-day simulation was analyzed in this study. Additional two sets of experiments were conducted in April 2019 and April 2018 for a better understanding of the physical mechanism of said sensitivity experiment.

The average modifications or decreases in the surface standard meteorological field for 2018 and 2019 are fairly close to those for the experiments conducted in 2020. The average correlation values for each standard meteorological field range from 0.89 to 0.92 during the phase of the experiment, and they are highly significant at the 0.05 level of significance. It may be deduced that a single day simulation is sufficient to accurately replicate each surface standard field for heat mitigation measures. In the supplementary information, average changes (experiment minus control) representing the 3-case study average (2018, 2019, and 2020) in net inflow radiation, 2-m ambient temperature, surface skin temperature, dew point temperature, relative humidity, PBL height are shown in Supporting Information S1 for daytime and nighttime (Figures S2–S7).

The difference in spatial and diurnal scale variability of the partition of urban surface energy balance and thermal balance (mainly 2-m ambient air temperature and surface skin temperature) was calculated for a three-member ensemble study by WRF-SLUCM. This ensemble study shows that the hourly average of April month in the 2019 and 2018 simulations reproduced almost similar results ($\pm$4 Wm^{-2}) for urban surface energy balance as well as urban thermal balance ($\pm$0.3°C) compared to 2020. The maximum reduction of sensible heat flux during peak hour average (14:00 LT) was 171.1 Wm^{-2} for CMs, 110.5 Wm^{-2} for GRs, 67.9 Wm^{-2}or VEG, 164.6 Wm^{-2} for CC, and 180.3 Wm^{-2} for super cool materials in the year of 2019 compared to control case. In 2018, the maximum reduction of sensible heat was 169.4 Wm^{-2} for CMs, 108.4 Wm^{-2} for GRs, 68.4 Wm^{-2} for VEG, 165.7 Wm^{-2} for CC, and 178.4 Wm^{-2} for SCMs respectively compare to control case. The rate of reduction of sensible heat flux for monthly average (hourly) values was close to the 1-day average (hourly) simulation for this experimental study. In the case of latent heat flux and heat storage, the same result was reproduced in a 2-day average simulation with slightly fluctuating between and within the year due to unforeseen atmospheric changes with the synoptic weather condition in pre-monsoon seasons. The ensemble study showed that the maximum decrease in the net inflow radiation from the urban surface was 242.2 Wm^{-2} for CMs, 147.3 Wm^{-2} for CC, and 223.4 Wm^{-2} for SCMs, but an increase of 39.3 Wm^{-2} for GRs and 47.6 Wm^{-2} for VEG compare to control case for 2019 simulation. For 2018 simulation, the rate of reduction of net inflow radiation from the urban surface was 249.5 Wm^{-2} for CMs, 152.3 Wm^{-2} for CC, and 227.6 Wm^{-2} for SCMs, but an increase of 38.8 Wm^{-2} for GRs and 42.3 Wm^{-2} for the VEG experiment. So, the energy balances of urban surface from different meteorological conditions simulation consistently produces nearly the same pattern of diurnal as well as spatial 2-day simulation as present in Section 4.1. The urban surface energy balance in 2019 and 2018 simulation results are given in Supporting Information S1 (Tables S1 and S2).

In this study, the impact of heat mitigation technologies on the surface meteorological field, 2-m ambient air temperature, and surface skin temperature were compared with the 2-day simulation. The maximum reduction of 2-m ambient air temperature was 1.3°C for CMs and VEG, 0.8°C for GRs, 1.2°C for CC, and 1.5°C for SCMs for the 2019 simulation. Based on the 2018 simulation, the maximum decrease of 2-m ambient temperature was 1.3°C, 0.6°C, 1.2°C, 1.1°C, and 1.4°C for CMs, GRs, VEG, CC, and SCMs experiments respectively over the urban domain compared to control case. This result shows that the 2-m ambient temperature is reasonably well estimated. In the case of surface skin temperature, the maximum decrease was 3.8°C for CMs, 2.3°C for GRs, 2.1°C for VEG, 3.9°C for CC, and 4°C for SCMs in 2019 simulation. In the 2018 simulation, the maximum reduction of surface skin temperature was 3.8°C for CMs, CC, and SCMs, 2.2°C for GRs, and 2.1°C for the VEG experiment compared to the control case. The diurnal profile of 2-m ambient temperature and surface skin temperature for consecutive year simulation (April for both years) are also presented in Supporting Information S1 (Tables S3 and S4). Different meteorological conditions simulation for the 2 years in the WRF-SLUCM model produced an almost consistent pattern of urban energy as well as thermal balance as compared with a 1-day simulation with the same physical parameterization process within an urban environment are presented in Section 4.2.

6. Discussions: Limitations, Impacts and Future Research

The primary drawback of the current study is the use of single-day simulations. Lower atmospheric processes cannot be well captured by a single-day simulation. However, because to a lack of long-term observed data over Kolkata, we conducted it for a single day-run with various meteorological conditions for two selected days in the month of April in 2018, 2019, and 2020. Further research can include longer time scales. Compared to meteorological and other climatological studies, there are very few studies on the impact of cool roofs or GRs and their combinations on the urban climate, especially in the tropics. As the air-quality effects of urban surface modification by heat mitigation measures are complex and, nonlinear, comprehensive emissions processing, meteorological and chemical transport models are needed to accurately determine potential impacts on air quality for policy-making purposes. The ambient pollutant concentrations will be affected due to the mixing height and ventilation (A. Sharma et al., 2016). Cool roofs can reduce temperature-dependent emissions of precursors to ozone (O_3) and particulate matter in urban areas by lowering ambient temperatures, resulting in a slower rate of volatile organic content evaporation and NOx emissions (Millstein & Menon, 2011). Cool materials might lead to meteorological modifications that may impact ozone and $PM_{2.5}$ concentrations besides having enhanced ultraviolet reflection (Epstein et al., 2017). Whether ozone ultimately increases or decreases in the most populated areas will depend on the relative importance of multiple physicochemical pathways, including ozone decreases from temperature reductions, ozone increases from reduced ventilation and mixing, and ozone increases from possible ultra-violet radiation increases.

When assessing the impacts of cool roofs, it is important to consider all the environmental and economic consequences, as benefits from a reduction in heat-related mortality may outweigh the increase in mortality from enhanced $PM_{2.5}$ pollution. Although there are other techniques to control ambient air pollution in urban areas through emission reduction policies, the availability of urban heat mitigation strategies is limited in tropical cities. Without a comprehensive analysis of all the benefits of cool roofs it would be a mistake to discourage this technology solely based on air quality alone. Although there are many studies on air quality changes due to mitigation strategies, there is limited research focused on tropical coastal cities. Future research addressing the effects of mitigation strategies on urban air quality parameters are needed, and are beyond the scope of the present research.

CMs and SCMs, as they reflect solar radiation, are likely to reduce vertical mixing and lower PBL heights, negatively impacting urban pollutant dispersion. The lower atmosphere increases pollution and creates additional health problems due to possible urban air quality deterioration in green fraction and reflective materials. The modification in the PBL as a result of the deployment of different mitigation strategies also impacts the temperature and moisture profiles over the urban areas and has potential impacts on cloud and precipitation processes. However, the latter topic of research is the subject of future work. Most of the recent studies have focused only on heatwave episodes or synoptic hot summer days, while the potential long-term (year or decade scale) effects of various mitigation strategies also need to be investigated, especially to understand the effects on precipitation processes (J. Liu & Niyogi, 2019; Patel et al., 2021).

Furthermore, highly reflective materials can reduce the moisture transported to the PBL, and subsequently, cities could be drier (Huang et al., 2023). In other words, GRs can append additional moisture to the PBL with extra latent heat flux and remove air pollutants through dry and wet depositions but entail a significant volume of water for regular irrigation to maintain cooling efficacy and plant activity, which is an added challenge for urban planners. Further, increased coagulation of pollutants with water vapor may create more health problems. Hence, it is challenging to answer the question "which heat mitigation technologies or strategies are suitable for improving thermal fields of the tropical coastal city?" given the multifaceted trade-offs in the energy-water-ecosystem-service nexus. For example, SCM will substantially decrease the cooling needs and thus will decrease the emission of pollutants and AH. On the other hand, GRs will increase the latent cooling load of buildings and can potentially increase pollutants and AH.

Additional consideration must also be made for the vertical thermodynamic profiles. For example, heat mitigation technologies will decrease the maximum convective available potential energy (CAPE) in the urban core and increase the spatio-temporal variability of CAPE (Houston & Niyogi, 2007), which entails that the local landscape modification can affect the regional convective precipitation pattern through land-atmosphere feedbacks (Oh & Sushama, 2021; Sati & Mohan, 2021). With the implementation of heat mitigation technologies, atmospheric

moisture is reduced; initially, convective precipitation could decrease over the core urban but enhanced downwind (J. Liu & Niyogi, 2019). This work is the subject of ongoing and future research.

Furthermore, we present a detailed spatio-temporal investigation of several simulated scenarios with a horizontal and vertical extent of PBL variables. The effect of heat mitigation technologies on convective urban rainfall can be measured with cloud microphysics retrieved from satellites and ground-based radars. Determining the real-time interaction between the relatively unexplored behavior of the PBL and air pollution is recommended for future model development, and is not within the scope of this study. No prior study presents holistic impacts of different available mitigation technologies on the surface, energy flux, and PBL dynamics. Most of the previous work has focused only on surface meteorological fields in other climates, with few exceptions (e.g., Brandi et al., 2021). The results presented here provide insight for atmospheric scientists and urban planners alike, enabling prioritization of the spectrum of heat mitigation strategies within a local context.

7. Conclusion

We studied the impact of the implementation of these scenarios on the regional urban energy budget, on the surface meteorological fields, atmospheric boundary layer dynamics and on sea breeze circulations. This study researched the regional impacts of different heat mitigation technologies on a tropical coastal city using the regional climate model (WRF-SLUCM). The study focused on a hot summer day when heatwaves prevailed. To allay the single-day simulations concerns, we have added two consecutive very hot summer days during the pre-monsoon month of April to assess how heat mitigation strategies as additional case studies, each of 48-hr duration in the year 2019 and 2018. These additional simulations demonstrate that our initial results are completely consistent with 2020 scenarios. These additional simulations indicate that our initially conclusions are indeed robust. With the physically based SLUCM, the WRF model efficiently captured the meteorological conditions prevalent over the urban area. One base case (control) and five additional numerical simulations (GRs, CMs, SCMs, VEG, i.e., increase in the vegetation fraction and “cool city-CC”) were studied. The modification of albedo, emissivity, and rooftop vegetation (roof only), to roof, wall, and ground alter the urban radiation balance.

The impacts of CMs, GRs, “cool cities,” and super-cool materials led to lowering the sensible heat, surface skin temperature, and ambient temperature. The increased roof albedo to 0.65 was as effective as the expansion to 100% GRs and CC for the present experiments under the tropical urban environment considered. However, increasing the localized "global" albedo from 0.20 to 0.96 caused a cool island effect and a decrease of the ambient temperature up to 1.6°C compared to the control case. On the other hand, GRs led to higher near-surface relative humidity due to enhanced evapotranspiration. The near-surface relative humidity increased in the CC experiments due to the combined effects of reflective materials and rooftop greening on the surface energy balance.

We showed that the impact of conventional CMs, GRs, vegetative surfaces, and CC on PBL is less notable during the daytime, possibly due to low reflectivity, solar radiation emissivity, and less evapotranspiration rooftop vegetation. However, super-cool materials could significantly lower the height of the PBL due to the considerable reduction of surface absorbed solar energy. In tropical Kolkata, cool and super-cool materials may be promising technologies to reduce the sensible heat flux by about 60%–80% (by ∼150–300 Wm^{-2}) compared to the control simulation. The difference of 2 m ambient air temperature between the control and experimental cases showed that the super-cool material simulation showed the largest regional influence for most experiments. The GRs experiment led to a decrease in $\Delta T_{ambient}$ of 0.88°C, as a result of rooftop gardening and transpiration.

The regional impacts of heat mitigation technologies have been evaluated using prognostic and diagnostic model-induced meteorological variables. The regional effect is greater for some heat mitigation scenarios than others. The study assessed ambient temperature, surface-specific and relative humidity impacts when the roofs, walls, and ground were covered with high albedo materials or the GRs reached a higher fraction. The changes in the vertical profiles of potential temperature indicate a more stable PBL over the urban areas for cool and super-cool materials compared to the GRs and CC scenario. These highly reflective cool and super-cool materials decreased the PBL height; the diurnal averaged decrease of the model diagnosed PBL height could reach more than 500–600 m over the urban area, although it depends on the physical processes of PBL during day and nighttime. The decrease in ambient temperature and increase in specific/relative humidity due to the urban

heat mitigation strategies extended from the urban surface to the top of the PBL. Simultaneously, the intersect phenomena occurred above the PBL due to significant decreases in the vertical wind speed.

The results revealed that cool and super-cool materials are efficient technologies to modify the lower atmosphere of the urban domain. However, the urban heat mitigation technologies can also reduce the vertical mixing over urban areas, may potentially degrading air quality in cities, in alignment with prior work in non-tropical cities (Brandi et al., 2021; Georgescu, 2015). Future research is ongoing to expand these results to more locations in different climates. To conclude, extensive but holistic approach has been undertaken on the cooling potential and local meteorological implications of surface and rooftop heat mitigation methods in tropical urban settings. We evaluated newly developed SCMs alongside other mitigating measures. Practioners may use the findings of this study to acquire a complete understanding of the predicted performance of surface and rooftop heat mitigation measures when applied city-wide to avert extreme urban heat and counteract its impacts on indoor thermal comfort and local thermodynamic efficiency (Ye & Niyogi, 2022).

Data Availability Statement

The software and data that support the findings of this study are openly available. The source code of WRF model Version 4.0.0 (Skamarock et al., 2021) [Software], available at (http://dx.doi.org/10.5065/1dfh-6p97). For forcing initial and boundary conditions of the WRF model, data are available in Research Data Archive (NCEP, 2015) at the National Center for Atmospheric Research, Computational and Information Systems Laboratory, Boulder, Colorado. [Datasets], available at (https://doi.org/10.5065/D65D8PWK). The in situ meteorological data for WRF model validation data (Weather Kolkata, 2018) [Datasets], available at (http://www.weatherkolkata.in/). To validate the PBL height with upper air Radiosonde data for VECC Calcutta Observations (Wyoming Weather Web, 1973) [Datasets], available at (http://weather.uwyo.edu/).

Acknowledgments
DN acknowledges the William Stamps Farish Chair through the Jackson School of Geosciences at University of Texas; and funding from NOAA NIHHIS NA21OAR4310146, NASA Interdisciplinary Sciences (IDS) Program (NNH19ZDA001N-IDS and 80NSSC20K1268), and DOE Urban Integrated Field Labs (IFL).

References

Aflaki, A., Mirnezhad, M., Ghaffarianhoseini, A., Ghaffarianhoseini, A., Omrany, H., Wang, Z.-H., & Akbari, H. (2017). Urban heat island mitigation strategies: A state-of-the-art review on Kuala Lumpur, Singapore and Hong Kong. *Cities*, *62*, 131–145. https://doi.org/10.1016/j.cities.2016.09.003

Akbari, H., Levinson, R., Konopaki, S., & Rainer, L. (2004). *Monitoring the energy-use effects of cool roofs on California commercial buildings (LBNL-54770)*. Lawrence Berkeley National Laboratory (LBNL). https://doi.org/10.2172/840985

Akbari, H., Pomerantz, M., & Taha, H. (2001). Cool surfaces and shade trees to reduce energy use and improve air quality in urban areas. *Solar Energy*, *70*(3), 295–310. https://doi.org/10.1016/S0038-092X(00)00089-X

Alapaty, K., Pleim, J. E., Raman, S., Niyogi, D. S., & Byun, D. W. (1997). Simulation of atmospheric boundary layer processes using local- and nonlocal-closure schemes. *Journal of Applied Meteorology*, *36*(3), 214–233. https://doi.org/10.1175/1520-0450(1997)036<0214:soablp>2.0.co;2

Alapaty, K., Seaman, N. L., Niyogi, D. S., & Hanna, A. F. (2001). Assimilating surface data to improve the accuracy of atmospheric boundary layer simulations. *Journal of Applied Meteorology*, *40*(11), 2068–2082. https://doi.org/10.1175/1520-0450(2001)040<2068:asdtit>2.0.co;2

Ali-Toudert, F., Djenane, M., Bensalem, R., & Mayer, H. (2005). Outdoor thermal comfort in the old desert city of Beni-Isguen, Algeria. *Climate Research*, *28*(3), 243–256. https://doi.org/10.3354/cr028243

Baklanov, A. A., Grisogono, B., Bornstein, R., Mahrt, L., Zilitinkevich, S. S., Taylor, P., et al. (2011). The nature, theory, and modeling of atmospheric planetary boundary layers. *Bulletin of the American Meteorological Society*, *92*(2), 123–128. https://doi.org/10.1175/2010BAMS2797.1

Baniassadi, A., Sailor, D. J., & Ban-Weiss, G. A. (2019). Potential energy and climate benefits of super-cool materials as a rooftop strategy. *Urban Climate*, *29*, 100495. https://doi.org/10.1016/j.uclim.2019.100495

Bao, H., Yan, C., Wang, B., Fang, X., Zhao, C. Y., & Ruan, X. (2017). Double-layer nanoparticle-based coatings for efficient terrestrial radiative cooling. *Solar Energy Materials and Solar Cells*, *168*, 78–84. https://doi.org/10.1016/j.solmat.2017.04.020

Bartesaghi-Koc, C., Haddad, S., Pignatta, G., Paolini, R., Prasad, D., & Santamouris, M. (2021). Can urban heat be mitigated in a single urban street? Monitoring, strategies, and performance results from a real scale redevelopment project. *Solar Energy*, *216*, 564–588. https://doi.org/10.1016/j.solener.2020.12.043

Bechtel, B., Demuzere, M., Sismanidis, P., Fenner, D., Brousse, O., Beck, C., et al. (2017). Quality of crowdsourced data on urban morphology—The human influence experiment (HUMINEX). *Urban Science*, *1*(2), 15. https://doi.org/10.3390/urbansci1020015

Brandi, A., Broadbent, A. M., Krayenhoff, E. S., & Georgescu, M. (2021). Influence of projected climate change, urban development and heat adaptation strategies on end of twenty-first century urban boundary layers across the Conterminous US. *Climate Dynamics*, *57*(3–4), 757–773. https://doi.org/10.1007/s00382-021-05740-w

Carlosena, L., Andueza, Á., Torres, L., Irulegi, O., Hernández-Minguillón, R. J., Sevilla, J., & Santamouris, M. (2021). Experimental development and testing of low-cost scalable radiative cooling materials for building applications. *Solar Energy Materials and Solar Cells*, *230*, 111209. https://doi.org/10.1016/j.solmat.2021.111209

Carlosena, L., Ruiz-Pardo, Á., Feng, J., Irulegi, O., Hernández-Minguillón, R. J., & Santamouris, M. (2020). On the energy potential of daytime radiative cooling for urban heat island mitigation. *Solar Energy*, *208*, 430–444. https://doi.org/10.1016/j.solener.2020.08.015

Charusombat, U., Niyogi, D., Kumar, A., Wang, X., Chen, F., Guenther, A., et al. (2010). Evaluating a new deposition velocity module in the noah land-surface model. *Boundary-Layer Meteorology*, *137*(2), 271–290. https://doi.org/10.1007/s10546-010-9531-y

Chatterjee, S., Khan, A., Dinda, A., Mithun, S., Khatun, R., Akbari, H., et al. (2019). Simulating micro-scale thermal interactions in different building environments for mitigating urban heat islands. *Science of the Total Environment*, *663*, 610–631. https://doi.org/10.1016/j.scitotenv.2019.01.299

Chen, F., & Dudhia, J. (2001). Coupling an advanced land surface-hydrology model with the Penn state-NCAR MM5 modeling system. Part I: Model implementation and sensitivity. *Monthly Weather Review*, *129*(4), 569–585. https://doi.org/10.1175/1520-0493(2001)129<0569:CAALSH>2.0.CO;2

Chen, F., Kusaka, H., Bornstein, R., Ching, J., Grimmond, C. S. B., Grossman-Clarke, S., et al. (2011). The integrated WRF/urban modelling system: Development, evaluation, and applications to urban environmental problems. *International Journal of Climatology*, *31*(2), 273–288. https://doi.org/10.1002/joc.2158

Chen, H., Ooka, R., Huang, H., & Tsuchiya, T. (2009). Study on mitigation measures for outdoor thermal environment on present urban blocks in Tokyo using coupled simulation. *Building and Environment*, *44*(11), 2290–2299. https://doi.org/10.1016/j.buildenv.2009.03.012

Chen, L., & Ng, E. (2013). Simulation of the effect of downtown greenery on thermal comfort in subtropical climate using PET index: A case study in Hong Kong. *Architectural Science Review*, *56*(4), 297–305. https://doi.org/10.1080/00038628.2012.684871

Chen, Z., Zhu, L., Raman, A., & Fan, S. (2016). Radiative cooling to deep sub-freezing temperatures through a 24-h day–night cycle. *Nature Communications*, *7*(1), 13729. https://doi.org/10.1038/ncomms13729

Cheng, C. Y., Cheung, K. K. S., & Chu, L. M. (2010). Thermal performance of a vegetated cladding system on facade walls. *Building and Environment*, *45*(8), 1779–1787. https://doi.org/10.1016/j.buildenv.2010.02.005

Ching, J., Aliaga, D., Mills, G., Masson, V., See, L., Neophytou, M., et al. (2019). Pathway using WUDAPT's Digital Synthetic City tool towards generating urban canopy parameters for multi-scale urban atmospheric modeling. *Urban Climate*, *28*, 100459. https://doi.org/10.1016/j.uclim.2019.100459

Chow, W. T. L., Brennan, D., & Brazel, A. J. (2012). Urban heat island research in Phoenix, Arizona: Theoretical contributions and policy applications. *Bulletin of the American Meteorological Society*, *93*(4), 517–530. https://doi.org/10.1175/BAMS-D-11-00011.1

De Munck, C., Lemonsu, A., Masson, V., Le Bras, J., & Bonhomme, M. (2018). Evaluating the impacts of greening scenarios on thermal comfort and energy and water consumptions for adapting Paris city to climate change. *Urban Climate*, *23*, 260–286. https://doi.org/10.1016/j.uclim.2017.01.003

Dudhia, J. (1989). Numerical study of convection observed during the winter monsoon experiment using a mesoscale two-dimensional model. *Journal of the Atmospheric Sciences*, *46*(20), 3077–3107. https://doi.org/10.1175/1520-0469(1989)046<3077:NSOCOD>2.0.CO;2

Dwivedi, A., & Mohan, B. K. (2018). Impact of green roof on micro climate to reduce Urban Heat Island. *Remote Sensing Applications: Society and Environment*, *10*, 56–69. https://doi.org/10.1016/j.rsase.2018.01.003

Emmanuel, R., Rosenlund, H., & Johansson, E. (2007). Urban shading—A design option for the tropics? A study in Colombo, Sri Lanka. *International Journal of Climatology*, *27*(14), 1995–2004. https://doi.org/10.1002/joc.1609

Epstein, S. A., Lee, S.-M., Katzenstein, A. S., Carreras-Sospedra, M., Zhang, X., Farina, S. C., et al. (2017). Air-quality implications of widespread adoption of cool roofs on ozone and particulate matter in southern California. *Proceedings of the National Academy of Sciences of the United States of America*, *114*(34), 8991–8996. https://doi.org/10.1073/pnas.1703560114

Express News Service. (2021). 2020 8th warmest year in India in 121 years: IMD. *The Indian Express*. Retrieved from https://indianexpress.com/article/india/2020-8th-warmest-year-in-india-in-121-years-imd-7132668/

Feng, J., Khan, A., Doan, Q.-V., Gao, K., & Santamouris, M. (2021). The heat mitigation potential and climatic impact of super-cool broadband radiative coolers on a city scale. *Cell Reports Physical Science*, *2*(7), 100485. https://doi.org/10.1016/j.xcrp.2021.100485

Freitas, E. D., Rozoff, C. M., Cotton, W. R., & Dias, P. L. S. (2007). Interactions of an urban heat island and sea-breeze circulations during winter over the metropolitan area of São Paulo, Brazil. *Boundary-Layer Meteorology*, *122*(1), 43–65. https://doi.org/10.1007/s10546-006-9091-3

Fung, K. Y., Yang, Z.-L., & Niyogi, D. (2022). Improving the local climate zone classification with building height, imperviousness, and machine learning for urban models. *Computational Urban Science*, *2*(1), 16. https://doi.org/10.1007/s43762-022-00046-x

Gentle, A. R., & Smith, G. B. (2015). A subambient open roof surface under the mid-summer sun. *Advanced Science*, *2*(9), 1500119. https://doi.org/10.1002/advs.201500119

Georgescu, M. (2015). Challenges associated with adaptation to future urban expansion. *Journal of Climate*, *28*(7), 2544–2563. https://doi.org/10.1175/JCLI-D-14-00290.1

Georgescu, M., Morefield, P. E., Bierwagen, B. G., & Weaver, C. P. (2014). Urban adaptation can roll back warming of emerging megapolitan regions. *Proceedings of the National Academy of Sciences of the United States of America*, *111*(8), 2909–2914. https://doi.org/10.1073/pnas.1322280111

Georgescu, M., Moustaoui, M., Mahalov, A., & Dudhia, J. (2013). Summer-time climate impacts of projected megapolitan expansion in Arizona. *Nature Climate Change*, *3*(1), 37–41. https://doi.org/10.1038/nclimate1656

Gilliam, R. C., & Pleim, J. E. (2010). Performance assessment of new land surface and planetary boundary layer physics in the WRF-ARW. *Journal of Applied Meteorology and Climatology*, *49*(4), 760–774. https://doi.org/10.1175/2009jamc2126.1

Gilliam, R. C., Raman, S., & Niyogi, D. D. S. (2004). Observational and numerical study on the influence of large-scale flow direction and coastline shape on sea-breeze evolution. *Boundary-Layer Meteorology*, *111*(2), 275–300. https://doi.org/10.1023/B:BOUN.0000016494.99539.5a

González, J. E., Ramamurthy, P., Bornstein, R. D., Chen, F., Bou-Zeid, E. R., Ghandehari, M., et al. (2021). Urban climate and resiliency: A synthesis report of state of the art and future research directions. *Urban Climate*, *38*, 100858. https://doi.org/10.1016/j.uclim.2021.100858

Hamdi, R., Degrauwe, D., & Termonia, P. (2012). Coupling the Town Energy Balance (TEB) scheme to an operational limited-area NWP model: Evaluation for a highly urbanized area in Belgium. *Weather and Forecasting*, *27*(2), 323–344. https://doi.org/10.1175/waf-d-11-00064.1

Hamdi, R., Duchêne, F., Berckmans, J., Delcloo, A., Vanpoucke, C., & Termonia, P. (2016). Evolution of urban heat wave intensity for the Brussels Capital Region in the ARPEGE-Climat A1B scenario. *Urban Climate*, *17*, 176–195. https://doi.org/10.1016/J.UCLIM.2016.08.001

Hamdi, R., Kusaka, H., Doan, Q.-V., Cai, P., He, H., Luo, G., et al. (2020). The state-of-the-art of urban climate change modeling and observations. *Earth Systems and Environment*, *4*(4), 631–646. https://doi.org/10.1007/s41748-020-00193-3

Houston, A. L., & Niyogi, D. (2007). The sensitivity of convective initiation to the lapse rate of the active cloud-bearing layer. *Monthly Weather Review*, *135*(9), 3013–3032. https://doi.org/10.1175/mwr3449.1

Huang, S., Gan, Y., Zhang, X., Chen, N., Wang, C., Gu, X., et al. (2023). Urbanization amplified asymmetrical changes of rainfall and exacerbated drought: Analysis over five urban agglomerations in the Yangtze River basin, China. *Earth's Future*, *11*(2). Portico. https://doi.org/10.1029/2022ef003117

Indian Institute of Technology Kharagpur, & Municipal Corporation. (2020). Weather Kolkata. Retrieved from http://weatherkolkata.in/

Jim, C. Y. (2015). Assessing climate-adaptation effect of extensive tropical green roofs in cities. *Landscape and Urban Planning*, *138*, 54–70. https://doi.org/10.1016/j.landurbplan.2015.02.014

Kain, J. S. (2004). The Kain–Fritsch convective parameterization: An update. *Journal of Applied Meteorology and Climatology*, *43*(1), 170–181. https://doi.org/10.1175/1520-0450(2004)043<0170:TKCPAU>2.0.CO;2

Khan, A., Akbari, H., Fiorito, F., Mithun, S., & Niyogi, D. (Eds.) (2022). *Global urban heat island mitigation*. https://doi.org/10.1016/c2020-0-02681-2

Khan, A., Carlosena, L., Feng, J., Khorat, S., Khatun, R., Doan, Q.-V., & Santamouris, M. (2022). Optically modulated passive broadband daytime radiative cooling materials can cool cities in summer and heat cities in winter. *Sustainability*, *14*(3), 1110. https://doi.org/10.3390/su14031110

Khan, A., Carlosena, L., Khorat, S., Khatun, R., Doan, Q.-V., Feng, J., & Santamouris, M. (2021). On the winter overcooling penalty of super cool photonic materials in cities. *Solar Energy Advances*, *1*, 100009. https://doi.org/10.1016/j.seja.2021.100009

Khan, A., & Chatterjee, S. (2016). Numerical simulation of urban heat island intensity under urban–suburban surface and reference site in Kolkata, India. *Modeling Earth Systems and Environment*, *2*(2), 71. https://doi.org/10.1007/s40808-016-0119-5

Khan, A., Khorat, S., Khatun, R., Doan, Q.-V., Nair, U. S., & Niyogi, D. (2021). Variable impact of COVID-19 lockdown on air quality across 91 Indian cities. *Earth Interactions*, *25*(1), 57–75. https://doi.org/10.1175/EI-D-20-0017.1

Krayenhoff, E. S., Broadbent, A. M., Zhao, L., Georgescu, M., Middel, A., Voogt, J. A., et al. (2021). Cooling hot cities: A systematic and critical review of the numerical modelling literature. *Environmental Research Letters*, *16*(5), 053007. https://doi.org/10.1088/1748-9326/abdcf1

Krayenhoff, E. S., Moustaoui, M., Broadbent, A. M., Gupta, V., & Georgescu, M. (2018). Diurnal interaction between urban expansion, climate change and adaptation in US cities. *Nature Climate Change*, *8*(12), 1097–1103. https://doi.org/10.1038/s41558-018-0320-9

Kusaka, H., Kondo, H., Kikegawa, Y., & Kimura, F. (2001). A simple single-layer urban canopy model for atmospheric models: Comparison with multi-layer and slab models. *Boundary-Layer Meteorology*, *101*(3), 329–358. https://doi.org/10.1023/A:1019207923078

Lee, T. R., & De Wekker, S. F. (2016). Estimating daytime planetary boundary layer heights over a valley from rawinsonde observations at a nearby airport: An application to the Page Valley in Virginia, United States. *Journal of Applied Meteorology and Climatology*, *55*(3), 791–809. https://doi.org/10.1175/jamc-d-15-0300.1

Li, X.-X., & Norford, L. K. (2016). Evaluation of cool roof and vegetations in mitigating urban heat island in a tropical city, Singapore. *Urban Climate*, *16*, 59–74. https://doi.org/10.1016/j.uclim.2015.12.002

Lim, X. (2019). The super-cool materials that send heat to space. *Nature*, *577*(7788), 18–21. https://doi.org/10.1038/d41586-019-03911-8

Lin, C.-Y., Chen, F., Huang, J. C., Chen, W.-C., Liou, Y.-A., Chen, W.-N., & Liu, S.-C. (2008). Urban heat island effect and its impact on boundary layer development and land–sea circulation over northern Taiwan. *Atmospheric Environment*, *42*(22), 5635–5649. https://doi.org/10.1016/j.atmosenv.2008.03.015

Lin, Y. L., Farley, R. D., & Orville, H. D. (1983). Bulk parameterization of the snow field in a cloud model. *Journal of Applied Meteorology and climatology*, *22*(6), 1065–1092.

Liu, C., Wu, Y., Wang, B., Zhao, C. Y., & Bao, H. (2019). Effect of atmospheric water vapor on radiative cooling performance of different surfaces. *Solar Energy*, *183*, 218–225. https://doi.org/10.1016/j.solener.2019.03.011

Liu, J., & Niyogi, D. (2019). Meta-analysis of urbanization impact on rainfall modification. *Scientific Reports*, *9*(1), 7301. https://doi.org/10.1038/s41598-019-42494-2

Mandal, J., Fu, Y., Overvig, A., Jia, M., Sun, K., Shi, N., et al. (2018). Hierarchically porous polymer coatings for highly efficient passive daytime radiative cooling. *Science*, *362*(6412), eaat9513. https://doi.org/10.1126/science.aat9513

Masson, V., Lemonsu, A., Hidalgo, J., & Voogt, J. (2020). Urban climates and climate change. *Annual Review of Environment and Resources*, *45*(1), 411–444. https://doi.org/10.1146/annurev-environ-012320-083623

Mellor, G. L., & Yamada, T. (1974). A hierarchy of turbulence closure models for planetary boundary layers. *Journal of the Atmospheric Sciences*, *31*(7), 1791–1806. https://doi.org/10.1175/1520-0469(1974)031<1791:AHOTCM>2.0.CO;2

Miao, S., & Chen, F. (2008). Formation of horizontal convective rolls in urban areas. *Atmospheric Research*, *89*(3), 298–304. https://doi.org/10.1016/j.atmosres.2008.02.013

Mills, G., Stewart, I. D., & Niyogi, D. (2022). The origins of modern urban climate science: Reflections on 'A numerical model of the urban heat island. *Progress in Physical Geography: Earth and Environment*, *46*(4), 649–656. https://doi.org/10.1177/03091333221107212

Millstein, D., & Menon, S. (2011). Regional climate consequences of large-scale cool roof and photovoltaic array deployment. *Environmental Research Letters*, *6*(3), 034001. https://doi.org/10.1088/1748-9326/6/3/034001

Mlawer, E. J., Taubman, S. J., Brown, P. D., Iacono, M. J., & Clough, S. A. (1997). Radiative transfer for inhomogeneous atmospheres: RRTM, a validated correlated-k model for the longwave. *Journal of Geophysical Research*, *102*(D14), 16663–16682. https://doi.org/10.1029/97JD00237

Mohan, M., & Bhati, S. (2011). Analysis of WRF model performance over subtropical region of Delhi, India. *Advances in Meteorology*, *2011*, 1–13. https://doi.org/10.1155/2011/621235

Morini, E., Castellani, B., Presciutti, A., Filipponi, M., Nicolini, A., & Rossi, F. (2017). Optic-energy performance improvement of exterior paints for buildings. *Energy and Buildings*, *139*, 690–701. https://doi.org/10.1016/j.enbuild.2017.01.060

Mughal, M. O., Li, X.-X., Yin, T., Martilli, A., Brousse, O., Dissegna, M. A., & Norford, L. K. (2019). High-resolution, multilayer modeling of Singapore's urban climate incorporating local climate zones. *Journal of Geophysical Research: Atmospheres*, *124*(14), 7764–7785. https://doi.org/10.1029/2018JD029796

Nadimpalli, R., Patel, P., Mohanty, U. C., Attri, S. D., & Niyogi, D. (2022). Impact of urban parameterization and integration of WUDAPT on the severe convection. *Computational Urban Science*, *2*(1), 41. https://doi.org/10.1007/s43762-022-00071-w

National Centers for Environmental Prediction/National Weather Service/NOAA/U.S. Department of Commerce. (2015). NCEP GFS 0.25 degree global forecast grids historical archive [Dataset]. UCAR/NCAR—Research Data Archive. https://doi.org/10.5065/D65D8PWK

Ng, E., Chen, L., Wang, Y., & Yuan, C. (2012). A study on the cooling effects of greening in a high-density city: An experience from Hong Kong. *Building and Environment*, *47*, 256–271. https://doi.org/10.1016/j.buildenv.2011.07.014

Niyogi, D., Holt, T., Zhong, S., Pyle, P. C., & Basara, J. (2006). Urban and land surface effects on the 30 July 2003 mesoscale convective system event observed in the southern Great Plains. *Journal of Geophysical Research*, *111*(D19), D19107. https://doi.org/10.1029/2005jd006746

Niyogi, D., Osuri, K. K., Busireddy, N. K. R., & Nadimpalli, R. (2020). Timing of rainfall occurrence altered by urban sprawl. *Urban Climate*, *33*, 100643. https://doi.org/10.1016/j.uclim.2020.100643

Niyogi, D., Pyle, P., Lei, M., Arya, S. P., Kishtawal, C. M., Shepherd, M., et al. (2011). Urban modification of thunderstorms: An observational storm climatology and model case study for the Indianapolis urban region. *Journal of Applied Meteorology and Climatology*, *50*(5), 1129–1144. https://doi.org/10.1175/2010JAMC1836.1

Niyogi, D. S., Raman, S., & Alapaty, K. (1999). Uncertainty in the specification of surface characteristics, part ii: Hierarchy of interaction-explicit statistical analysis. *Boundary-Layer Meteorology*, *91*(3), 341–366. https://doi.org/10.1023/a:1002023724201

Oh, S.-G., & Sushama, L. (2021). Urban-climate interactions during summer over eastern North America. *Climate Dynamics*, *57*(11), 3015–3028. https://doi.org/10.1007/s00382-021-05852-3

Patel, P., Jamshidi, S., Nadimpalli, R., Aliaga, D. G., Mills, G., Chen, F., et al. (2022). Modeling large-scale heatwave by incorporating enhanced urban representation. *Journal of Geophysical Research: Atmospheres*, *127*(2). e2021JD035316. https://doi.org/10.1029/2021jd035316

Patel, P., Karmakar, S., Ghosh, S., Aliaga, D. G., & Niyogi, D. (2021). Impact of green roofs on heavy rainfall in tropical, coastal urban area. *Environmental Research Letters*, *16*(7), 074051. https://doi.org/10.1088/1748-9326/ac1011

Patel, P., Karmakar, S., Ghosh, S., & Niyogi, D. (2020). Improved simulation of very heavy rainfall events by incorporating WUDAPT urban land use/land cover in WRF. *Urban Climate*, *32*, 100616. https://doi.org/10.1016/j.uclim.2020.100616

Pelliccioni, A., Monti, P., & Leuzzi, G. (2016). Wind-speed profile and roughness sublayer depth modelling in urban boundary layers. *Boundary-Layer Meteorology*, *160*(2), 225–248. https://doi.org/10.1007/s10546-016-0141-1

Pleim, J. E. (2007). A combined local and nonlocal closure model for the atmospheric boundary layer. Part II: Application and evaluation in a mesoscale meteorological model. *Journal of Applied Meteorology and Climatology*, *46*(9), 1396–1409. https://doi.org/10.1175/jam2534.1

Raman, S., Templeman, B., Templeman, S., Holt, T., Murthy, A. B., Singh, M. P., et al. (1990). Structure of the Indian southwesterly pre-monsoon and monsoon boundary layers: Observations and numerical simulation. *Atmospheric Environment, Part A: General Topics*, *24*(4), 723–734. https://doi.org/10.1016/0960-1686(90)90273-P

Routray, A., Mohanty, U. C., Rizvi, S. R. H., Niyogi, D., Osuri, K. K., & Pradhan, D. (2010). Impact of Doppler weather radar data on numerical forecast of Indian monsoon depressions. *Quarterly Journal of the Royal Meteorological Society*, *136*(652), 1836–1850. https://doi.org/10.1002/qj.678

Santamouris, M. (2014a). Cooling the cities—A review of reflective and green roof mitigation technologies to fight heat island and improve comfort in urban environments. *Solar Energy*, *103*, 682–703. https://doi.org/10.1016/j.solener.2012.07.003

Santamouris, M. (2014b). On the energy impact of urban heat island and global warming on buildings. *Energy and Buildings*, *82*, 100–113. https://doi.org/10.1016/j.enbuild.2014.07.022

Santamouris, M. (2020). Recent progress on urban overheating and heat island research. Integrated assessment of the energy, environmental, vulnerability and health impact. Synergies with the global climate change. *Energy and Buildings*, *207*, 109482. https://doi.org/10.1016/j.enbuild.2019.109482

Santamouris, M., Cartalis, C., Synnefa, A., & Kolokotsa, D. (2015). On the impact of urban heat island and global warming on the power demand and electricity consumption of buildings—A review. *Energy and Buildings*, *98*, 119–124. https://doi.org/10.1016/j.enbuild.2014.09.052

Santamouris, M., & Feng, J. (2018). Recent progress in daytime radiative cooling: Is it the air conditioner of the future? *Buildings*, *8*(12), 168. https://doi.org/10.3390/buildings8120168

Santamouris, M., & Osmond, P. (2020). Increasing green infrastructure in cities: Impact on ambient temperature, air quality and heat-related mortality and morbidity. *Buildings*, *10*(12), 233. https://doi.org/10.3390/buildings10120233

Santamouris, M., & Yun, G. Y. (2020). Recent development and research priorities on cool and super cool materials to mitigate urban heat island. *Renewable Energy*, *161*, 792–807. https://doi.org/10.1016/j.renene.2020.07.109

Sati, A. P., & Mohan, M. (2021). Impact of urban sprawls on thunderstorm episodes: Assessment using WRF model over central-national capital region of India. *Urban Climate*, *37*, 100869. https://doi.org/10.1016/j.uclim.2021.100869

Schmid, P., & Niyogi, D. (2012). A method for estimating planetary boundary layer heights and its application over the ARM southern great plains site. *Journal of Atmospheric and Oceanic Technology*, *29*(3), 316–322. https://doi.org/10.1175/jtech-d-11-00118.1

Shaffer, S. R., Chow, W. T. L., Georgescu, M., Hyde, P., Jenerette, G. D., Mahalov, A., et al. (2015). Multiscale modeling and evaluation of urban surface energy balance in the Phoenix metropolitan area. *Journal of Applied Meteorology and Climatology*, *54*(2), 322–338. https://doi.org/10.1175/JAMC-D-14-0051.1

Sharma, A., Conry, P., Fernando, H. J. S., Hamlet, A. F., Hellmann, J. J., & Chen, F. (2016). Green and cool roofs to mitigate urban heat island effects in the Chicago metropolitan area: Evaluation with a regional climate model. *Environmental Research Letters*, *11*(6), 064004. https://doi.org/10.1088/1748-9326/11/6/064004

Skamarock, W. C., Klemp, J. B., Dudhia, J., Gill, D. O., Liu, Z., Berner, J., et al. (2021). A description of the advanced research WRF model version 4.3 (No. NCAR/TN-556+STR) [Software]. https://doi.org/10.5065/1dfh-6p97

Song, J., & Wang, Z.-H. (2015). Interfacing the urban land–atmosphere system through coupled urban canopy and atmospheric models. *Boundary-Layer Meteorology*, *154*(3), 427–448. https://doi.org/10.1007/s10546-014-9980-9

Song, J., Wang, Z.-H., & Wang, C. (2018). The regional impact of urban heat mitigation strategies on planetary boundary layer dynamics over a semiarid city. *Journal of Geophysical Research: Atmospheres*, *123*(12), 6410–6422. https://doi.org/10.1029/2018JD028302

Stull, R. B. (1988). *An introduction to boundary layer meteorology*. Springer Science & Business Media.

Swain, M., Nadimpalli, R., Das, A. K., Mohanty, U. C., & Niyogi, D. (2023). Urban modification of heavy rainfall: A model case study for Bhubaneswar urban region. *Computational Urban Science*, *3*(1), 2. https://doi.org/10.1007/s43762-023-00080-3

Takebayashi, H., & Moriyama, M. (2007). Surface heat budget on green roof and high reflection roof for mitigation of urban heat island. *Building and Environment*, *42*(8), 2971–2979. https://doi.org/10.1016/j.buildenv.2006.06.017

Tan, C. L., Wong, N. H., Tan, P. Y., Jusuf, S. K., & Chiam, Z. Q. (2015). Impact of plant evapotranspiration rate and shrub albedo on temperature reduction in the tropical outdoor environment. *Building and Environment*, *94*, 206–217. https://doi.org/10.1016/j.buildenv.2015.08.001

Tewari, K., Tewari, M., & Niyogi, D. (2023). Need for considering urban climate change factors on stroke, neurodegenerative diseases, and mood disorders studies. *Computational Urban Science*, *3*(1), 4. https://doi.org/10.1007/s43762-023-00079-w

Wang, Y., Li, Y., Sabatino, S. D., Martilli, A., & Chan, P. W. (2018). Effects of anthropogenic heat due to air-conditioning systems on an extreme high temperature event in Hong Kong. *Environmental Research Letters*, *13*(3), 034015. https://doi.org/10.1088/1748-9326/aaa848

Weather Kolkata. (2018). Live rainfall and flood monitoring [Dataset]. Retrieved from http://www.weatherkolkata.in/

Wong, K. V., Paddon, A., & Jimenez, A. (2013). Review of world urban heat islands: Many linked to increased mortality. *Journal of Energy Resources Technology*, *135*(2), 022101. https://doi.org/10.1115/1.4023176

Wyoming Weather Web. (1973). Upper air data: Soundings, upper air maps, and balloon trajectory forecasts [Dataset]. Retrieved from http://weather.uwyo.edu/upperair/

Yang, L., Smith, J., & Niyogi, D. (2019). Urban impacts on extreme monsoon rainfall and flooding in complex terrain. *Geophysical Research Letters*, *46*(11), 5918–5927. https://doi.org/10.1029/2019gl083363

Ye, X., & Niyogi, D. (2022). Resilience of human settlements to climate change needs the convergence of urban planning and urban climate science. *Computational Urban Science*, *2*(1), 6. https://doi.org/10.1007/s43762-022-00035-0

Zhai, Y., Ma, Y., David, S. N., Zhao, D., Lou, R., Tan, G., et al. (2017). Scalable-manufactured randomized glass-polymer hybrid metamaterial for daytime radiative cooling. *Science*, *355*(6329), 1062–1066. https://doi.org/10.1126/science.aai7899

Zhang, C. L., Chen, F., Miao, S. G., Li, Q. C., Xia, X. A., & Xuan, C. Y. (2009). Impacts of urban expansion and future green planting on summer precipitation in the Beijing metropolitan area. *Journal of Geophysical Research*, *114*(D2), D02116. https://doi.org/10.1029/2008JD010328

Zhang, D.-L., Shou, Y.-X., Dickerson, R. R., & Chen, F. (2011). Impact of upstream urbanization on the urban heat island effects along the Washington–Baltimore corridor. *Journal of Applied Meteorology and Climatology*, *50*(10), 2012–2029. https://doi.org/10.1175/JAMC-D-10-05008.1

Zheng, Y., Alapaty, K., Herwehe, J. A., Del Genio, A. D., & Niyogi, D. (2016). Improving high-resolution weather forecasts using the weather research and forecasting (WRF) model with an updated Kain–Fritsch scheme. *Monthly Weather Review*, *144*(3), 833–860. https://doi.org/10.1175/mwr-d-15-0005.1

Zhao, B., Hu, M., Ao, X., & Pei, G. (2019). Performance evaluation of daytime radiative cooling under different clear sky conditions. *Applied Thermal Engineering*, *155*, 660–666. https://doi.org/10.1016/j.applthermaleng.2019.04.028

Zhong, H., Zhang, P., Li, Y., Yang, X., Zhao, Y., & Wang, Z. (2020). Highly solar-reflective structures for daytime radiative cooling under high humidity. *ACS Applied Materials & Interfaces*, *12*(46), 51409–51417. https://doi.org/10.1021/acsami.0c14075